Transportation Research Part C 152 (2023) 104158

Contents lists available at ScienceDirect

Transportation Research Part C

journal homepage: www.elsevier.com/locate/trc

Dynamic ride-sourcing systems for city-scale networks - Part I: Matching design and model formulation and validation

Mohsen Ramezani *, Amir Hosein Valadkhani

The University of Sydney, School of Civil Engineering, Sydney, Australia

ARTICLE INFO

Keywords:
E-hailing
Transportation network company (TNC)
Taxi
Two-sided markets
Shared mobility
Dynamic bilateral matching

ABSTRACT

The ubiquity of smart devices enables the foundation for emerging fast-growing ride-sourcing companies that challenge traditional taxi services. Two design aspects of on-demand mobility systems are: (i) the matching mechanism between idle ride-sourcing vehicles and passenger travel requests (i.e., vehicle–passenger matching) and (ii) the repositioning mechanism of idle vehicles. In this paper, we propose a macroscopic non-equilibrium dynamic model of ride-sourcing systems with capabilities of investigating the efficiency of vehicle–passenger matching and idle vehicle repositioning methods. A spatio-temporal vehicle–passenger matching method is introduced to determine dynamically and jointly the matching time instances and maximum matching distances to minimize passengers' waiting time (i.e., from the travel request until the pickup) while considering the network congestion levels. Designing a controller for repositioning idle vehicles to balance vehicle supply and passenger travel demand based on the proposed model is scrutinized in the companion paper (Part II). The accuracy of the proposed model and the performance of the matching method under noticeable variations of traffic congestion and passenger travel requests are investigated with microsimulation. The results demonstrate the accuracy of the model in predicting the evolution of the number of ride-sourcing vehicles in different states (idle, transferred, dispatched, and occupied) and passengers (waiting and assigned) in each region of the network. Furthermore, the effectiveness of the proposed matching method is demonstrated by the decrease in the waiting times of ride-sourcing vehicles and passengers.

1. Introduction

Advancements in information and communication technologies improve the convenience and affordability of ride-sourcing services which lead to the growing demand and use of these services. Ride-sourcing service providers such as Uber, DiDi, and Lyft provide on-demand point-to-point services for passengers through an online platform with a fleet of vehicles owned by self-scheduled drivers. The platforms (service providers) generally have goals such as profit maximization and/or reducing passenger waiting times to ensure a satisfactory level of service. The platforms have tools such as vehicle–passenger matching technology and idle vehicle repositioning (transferring) to achieve these objectives. In this paper, we introduce a dynamic non-equilibrium macro-model as a set of first-order differential equations to represent the dynamics of a ride-sourcing system. Moreover, we develop a vehicle–passenger matching method that adaptively changes the matching interval and the maximum matching distance (i.e., discarding vehicle–passenger matches whose distance is longer than the maximum matching distance) to minimize passengers' waiting time. A controller for dynamic idle vehicle repositioning based on the proposed model is developed in the companion paper (Part II).

* Corresponding author.
E-mail address: mohsen.ramezani@sydney.edu.au (M. Ramezani).

https://doi.org/10.1016/j.trc.2023.104158
Received 23 December 2022; Received in revised form 27 April 2023; Accepted 29 April 2023
Available online 15 May 2023

Modeling ride-sourcing systems exhibit traits of modeling taxi services. They are studied extensively with the focus of *equilibrium* analysis which reflects the stable steady-state behavior of the system. The initial steps were taken by equilibrium-based macroscopic models in Manski and Wright (1967), Orr (1969) and Douglas (1972). Later, in Yang and Wong (1998), a stationary model is established to formulate movements of cruising taxis. This model is further developed by considering the effect of congestion and passenger demand elasticity in Wong et al. (2001). The steady-state effect of bilateral taxi-passenger searching and meeting behavior at the equilibrium point is studied in Wong et al. (2005) and Yang et al. (2010b). In Wong et al. (2015), a two-stage equilibrium-based model is proposed to predict zonal and circulating movements of cruising taxis. In Yang et al. (2010a) and Yang and Yang (2011), the effect of search friction between vacant taxis and passengers on the equilibrium of the taxi system is scrutinized. A Ride-sourcing market is studied in Zha et al. (2016) by proposing an equilibrium-based macroscopic model to capture the taxi-passenger meeting dynamics with an external matching function. An equilibrium model in a hybrid market with the coexistence of cruising taxi and ride-sourcing systems is investigated in Qian and Ukkusuri (2017). Ramezani and Nourinejad (2018) initiates non-equilibrium-based modeling of cruising taxi systems and proposes a predictive controller to relocate the vacant taxis. A non-equilibrium model for a ride-sourcing market with a predictive controller is proposed to maximize the overall profit in Nourinejad and Ramezani (2019).

One dominant factor that affects the quality of service of ride-sourcing systems is the vehicle–passenger matching method. Among the recent studies that address vehicle–passenger matching, Santi et al. (2014) and Vazifeh et al. (2018) focus on high-capacity vehicle–passenger matching. Zhan et al. (2016) uses bipartite matching to evaluate the efficiency of taxi systems in terms of optimal matching and trip integration. A driver-rider matching scheme in a ride-sharing system is proposed in Wang et al. (2017) to minimize total system-wide vehicle miles. Zha et al. (2018) proposes an aggregate matching model to facilitate the analysis of market equilibrium and spatial pricing. The bipartite graph approach is utilized in Dandl et al. (2019) to propose a static strategy to jointly match autonomous vehicles (AVs) to user requests and reposition AVs. In Hörl et al. (2019), a large-scale agent-based simulation of vehicle fleet management for dispatching and repositioning is studied. A data-driven dispatching method for autonomous taxi systems is proposed in Hu and Dong (2020) to reduce the empty travel distance of autonomous taxis. Chen et al. (2021) develops a decentralized cooperative cruising method for autonomous ride-sourcing fleets without communications between the vehicles and the central dispatcher. Two common traits of most matching methods are assuming unlimited matching distance and fixed matching frequency. This paper tackles these two issues.

The effect of vehicle–passenger matching with unlimited radius has been empirically observed and theoretically analyzed in Castillo et al. (2017), Xu et al. (2020) and Zhang et al. (2019). The instantaneous joint effect of matching radius and matching interval in vehicle–passenger matching is studied in Yang et al. (2020) in a static way. In these articles, the matching interval is considered fixed and known and is obtained based on the current number of idle vehicles and waiting passengers. This neglects the intertwined effects between the predicted value of the matching interval (i.e., successive matching instances), the instantaneous spatial distribution of idle vehicles and waiting passengers, and the predicted value of average vehicle–passenger matching distance/time. To get more insight into the literature of shared mobility, interested readers can further refer to Salanova et al. (2011), Agatz et al. (2012), Ho et al. (2018) and Wang and Yang (2019).

Equilibrium-based modeling of ride-sourcing systems, which is common in literature, considers only the steady-state behavior of the system and does not consider the temporal variation of the systems' states (e.g., the number of vehicles and passengers). Furthermore, there are challenges to the existence, uniqueness, and finite-time reachability of equilibrium points of nonlinear dynamic ride-sourcing models. In this study, we propose a macroscopic non-equilibrium model to dynamically track different states of passengers and vehicles in a ride-sourcing system with the potential (i) to consider dynamic vehicle–passenger matching and (ii) to reposition idle vehicles. The model is built upon the augmented Cobb–Douglas matching function (Lagos, 2000) and Macroscopic Fundamental Diagrams (MFDs) (Geroliminis and Daganzo, 2008). Impatient passengers and drivers are included in the model by defining stochastic cancellation thresholds. Furthermore, to optimize expected passengers' waiting time, we propose a vehicle–passenger matching method to *dynamically* determine (i) the next matching time instance (enabling time-varying matching frequency) and (ii) the maximum matching distance to discard long-distance matchings (avoiding wild goose chase problem and letting vehicles to remain idle for repositioning).[1] Moreover, the proposed method considers the network congestion level, the predictions of the system's state in the short-term future, and the joint effect of optimum matching interval and maximum matching distance. The advantages of the matching method and the model's validity are investigated via a developed microsimulation benchmark. In Part II, a Nonlinear Model Predictive Controller (NMPC) is designed based on the model developed in this paper to proactively and dynamically reposition idle vehicles to suppress the spatial imbalance between idle vehicles (supply) and waiting passengers (demand).

The remainder of the article is organized as follows. In Section 2, we elaborate on different states of ride-sourcing vehicles and passengers in the ride-sourcing system. Also, we illustrate how the proposed model comprises matching and transferring in Section 2. In Section 3, the proposed adaptive spatio-temporal matching algorithm for dispatching idle ride-sourcing vehicles to waiting passengers is presented in detail. The proposed non-equilibrium macroscopic model is introduced in Section 4. Section 5 is devoted to assessing the performance of the proposed adaptive spatio-temporal matching method and illustrating the model's accuracy using microsimulation experiments. Finally, the article is concluded in Section 6.

[1] If the matching policy allows vehicles to be unassigned from requests and/or requests to be unassigned from vehicles, as the system evolves, the wild goose chase problem will be effectively immaterial (Hyland and Mahmassani, 2018). This policy would apply perfectly in a homogeneous fleet such as an AV fleet. However, this policy might be less practical today with the current composition of human-driven vehicles in TNCs with different vehicle quality (e.g., cleanness), driver experience, rating system, and safety issues (communicating the make, model, and registration number of the assigned vehicle and the name of the driver).

2. Preliminaries

This section defines terminologies used in this article for representing ride-sourcing vehicles and passengers states. Furthermore, we depict the schema of the proposed ride-sourcing system and describe its components and their interactions.

2.1. State definition

We design a *ride-sourcing system* as a centralized system for dispatching ride-sourcing vehicles to passengers' origin location and transferring the idle vehicles to the areas with a higher possibility of finding passengers. Let us assume an urban network that is partitioned into a few regions. We define four states for the ride-sourcing vehicles (i.e., idle, dispatched, transferred, and occupied) and three states for the passengers (i.e., waiting, assigned, and on-board). The four states of ride-sourcing vehicles are as follows:

(i) *Idle ride-sourcing vehicle* refers to a vacant vehicle that is not assigned to any passenger's travel request. It cruises randomly (or parks) until receiving a pick-up or transferring command from the ride-sourcing system. The number of idle ride-sourcing vehicles in Region i at time t is denoted as $c_i^{\mathrm{I}}(t)$.

(ii) *Dispatched ride-sourcing vehicle* is a vacant vehicle assigned to a passenger's travel request. It is sent to the passenger's location through the path recommended by the ride-sourcing system. The dispatched vehicles are not allowed to pick up other passengers along the recommended path. The number of dispatched ride-sourcing vehicles in Region i at time t is denoted as $c_i^{\mathrm{D}}(t)$.

(iii) *Transferred ride-sourcing vehicle* is a vacant vehicle sent to a location with an excess of passenger travel requests through the path recommended by the ride-sourcing system. Transferred vehicles are not assigned to any passenger's travel request. (Note that the system considers transferred vehicles in the pool of vehicles that can be assigned to unmatched passengers. Once such matching happens the vehicle state becomes dispatched). They balance the vehicle supply and travel request demand in different regions of the network. The ride-sourcing system can assign them to passengers' travel requests before reaching the hot-spot locations. The number of transferred vehicles in Region i at time t is denoted as $c_i^{\mathrm{T}}(t)$.

(iv) *Occupied ride-sourcing vehicle* is a vehicle servicing a passenger. We assume each vehicle services only one passenger or one group of passengers with the same origin and destination. The number of occupied vehicles in Region i at time t is denoted as $c_i^{\mathrm{O}}(t)$.

The three passenger's states are as:

(i) *Waiting passenger* refers to a passenger who has requested a ride, but she/he is not assigned to any ride-sourcing vehicle yet. The number of waiting passengers in Region i at time t is denoted as $p_i^{\mathrm{W}}(t)$.

(ii) *Assigned passenger* is a passenger who is not picked up by a vehicle, but a dispatched ride-sourcing vehicle is assigned to her/him. The number of assigned passengers in Region i at time t is denoted as $p_i^{\mathrm{A}}(t)$.

(iii) *On-board passenger* is a passenger picked up by a vehicle, but she/he has not reached her/his destination. The number of on-board passengers in Region i at time t is equal to the number of occupied vehicles in Region i at time t.

2.2. State transitions

Consider the movements of an *idle ride-sourcing vehicle* in a network that is divided into several regions. Once a *waiting passenger* is matched with an idle vehicle, the vehicle becomes *dispatched* and the passenger becomes *assigned*. Then, the dispatched ride-sourcing vehicle starts traveling towards the passenger's pick-up location with the path recommended by the ride-sourcing system. Once the dispatched vehicle reaches the location of the assigned passenger, the vehicle and passenger become *occupied* and *on-board*, respectively. Once the occupied vehicle reaches the on-board passenger's destination, the vehicle's state is changed to idle.

An idle ride-sourcing vehicle might be requested to reposition to other regions with an excess number of waiting passengers to balance the vehicle sources and passengers' travel demand. If the ride-sourcing system determines such region(s), a number of idle vehicles become *transferred* and will be guided to travel to that region(s). Note that the system considers transferred vehicles in the pool of vehicles that can be assigned to unmatched passengers (while transferring). If the transferred vehicle is not assigned to any passenger while traveling, it becomes idle again once it reaches the recommended transferring location.

To reflect reality more precisely, we assume if an idle ride-sourcing vehicle remains idle for an extended period, the driver leaves the ride-sourcing system. In addition, if a waiting or an assigned passenger is not picked up for a long time, the passenger cancels the travel request and quits the ride-sourcing service for other travel choices. When an assigned passenger cancels their travel request, the ride-sourcing vehicle matched to the passenger becomes idle.

Fig. 1 illustrates the state diagrams of vehicles and passengers in the ride-sourcing system. The dotted lines emphasize the vehicle's/passenger's state changes instantaneously without a physical trip (e.g., the state of an idle ride-sourcing vehicle becomes transferred once the driver receives the transfer command from the ride-sourcing system). The solid lines reflect a physical trip in the network (e.g., the dispatched vehicle must reach the assigned passenger's location to become occupied).

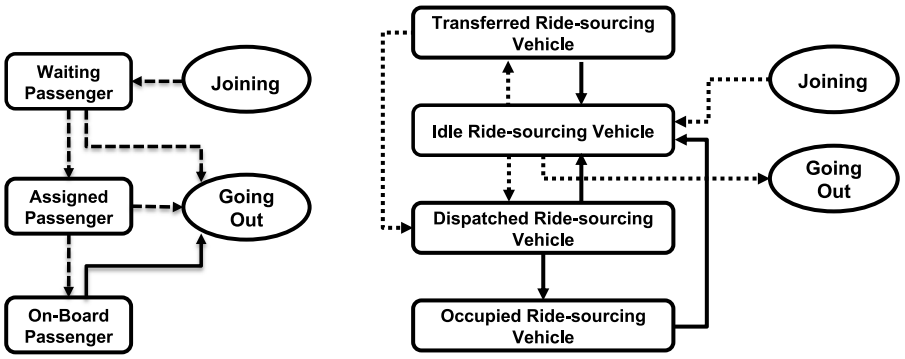

Fig. 1. State diagram of ride-sourcing systems' agents: (a) passengers and (b) ride-sourcing vehicles. Impatient passengers cancel their trips and leave if (i) they wait for more than a stochastic threshold or (ii) the assigned vehicle does not pick up the matched passenger before their pickup threshold. The second scenario also affects the dispatched vehicles and changes their state to idle.

2.3. Proposed schema

Interconnections between *plant* (i.e., traffic network), *model*, *dispatching subsystem*, and *transfer subsystem* are depicted in Fig. 2. The dispatching subsystem matches idle/transferred ride-sourcing vehicles and waiting passengers as two independent sets dynamically such that a subset of the idle/transferred vehicles are dispatched to minimize the total cruising time. It includes optimal myopic matching and adaptive spatio-temporal filtering methods. The former minimizes total matching distances with an assumption of maximal matching between the two independent sets, i.e., idle/transferred ride-sourcing vehicles and waiting passengers. The latter method obtains the result of the optimal myopic matching to minimize the total passengers' waiting time prediction to set dynamically and jointly: (i) the optimum next matching instance and (ii) the optimum upper bound of the matching distance between idle/transferred vehicles and waiting passengers at the current instance to avoid long-distance matchings.

The transfer subsystem has two components: *Transferred Ride-sourcing Controller* and *Link-Level Allocation*. The main component of the transfer subsystem is a macroscopic controller that dynamically recommends inter-regional movements of idle ride-sourcing vehicles in the network to balance the vehicles' supply and waiting passengers in the network. We propose a Nonlinear Model Predictive (NMPC) controller for repositioning idle vehicles in Part II of this study.

Link-Level Allocation translates the aggregated rate of idle vehicles in Region i that is recommended to be transferred to Region j (i.e., the output of the transfer controller) to disaggregated (vehicle-level) commands. It (i) selects a subset from the idle vehicles in Region i (based on their current locations and the accumulative time that they have been idle), (ii) assigns a link in Region j to each selected idle vehicle based on the location of the waiting passengers in Region j, and (iii) determines the shortest distance path by using Dijkstra's algorithm for each selected idle vehicle to reach the designated transferred link. The frequency of triggering transfer and dispatching subsystems are independent of each other. More details of the Transfer Subsystem are investigated in Part II of this study.

3. Dispatching subsystem

The dispatching subsystem includes optimal myopic and adaptive spatio-temporal filtering methods. It dynamically determines the optimum maximum matching distance and the next matching instance to minimize passengers' waiting time. At each matching instance, it considers the location of the waiting passengers and idle/transferred ride-sourcing vehicles, as well as the aggregated short-term prediction of the arrival rate of new passengers and idle/transferred vehicles. The optimal myopic method is first applied to match the waiting passengers and idle/transferred vehicles minimizing the total dispatch distance. Then the optimum maximum matching distance is determined to filter the long-distance matchings. Lastly, the optimum next matching instance is established to minimize passenger's waiting time. In Section 3.1, the optimal myopic method is explained that is built upon the maximum matching problem of a bipartite graph. It is a classic problem and has been widely studied in the literature, e.g., Agatz et al. (2011), Zhan et al. (2016), Vazifeh et al. (2018) and Yang and Ramezani (2023). Section 3.2 introduces the proposed method for finding the optimum matching intervals and maximum matching distances.

3.1. Optimal myopic matching

The optimal matching between idle/transferred ride-sourcing vehicles and waiting passengers at every matching instance is determined by solving the minimum weighted matching problem for a bipartite graph. It minimizes the total matching distances between idle/transferred vehicles and waiting passengers (equivalently, pickup times). We construct the problem as a bipartite graph by considering, (i) V_1 as the set of idle and transferred vehicles, (ii) V_2 as the set of the waiting passengers, and (iii) E as the edges

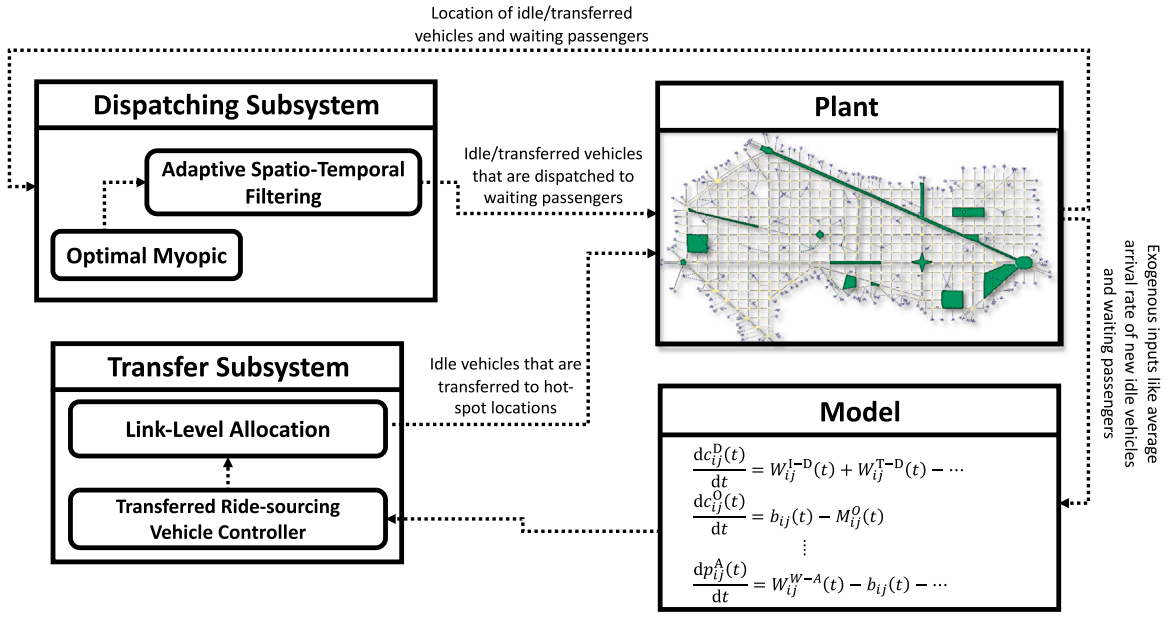

Fig. 2. Schematic of the proposed ride-sourcing system. The Dispatching subsystem matches the idle/transferred vehicles to the waiting passengers. The Dispatching Subsystem obtains the required information directly from the plant. The Model is utilized in Transfer Subsystem to predict the effect of idle vehicle repositioning on the future state of the ride-sourcing system. The output of the transfer subsystem is the idle vehicles that are altered to transferred vehicles and are guided to designated locations with excess passengers.

connecting each element of V_1 to V_2. The sets of V_1 and V_2 are disjoint and independent. The weight of each edge, $w(e)$, is the distance between the idle/transferred ride-sourcing vehicle and the waiting passenger. We obtain the minimum weighted matching for the bipartite graph using the integer linear programming method:

$$\begin{aligned} \text{minimize} \quad & \sum_{e\in E} x_e w(e) \\ \text{s.t.} \quad & \sum_{e\sim v} x_e \le 1 \quad \forall v \in \{V_1 \cup V_2\} \quad \& \quad \forall e \in E, \\ & \sum_{e\in E} x_e = \min(\|V_1\|, \|V_2\|) \\ & x_e \in \{0,1\} \qquad \forall e \in E, \end{aligned} \tag{1}$$

where $w(e)$ is the weight of each edge $e \in E$, $e \sim v$ denotes e is an incident on v, and $\|V_1\|$ denotes the size of set V_1. Eq. (1) requires the number of matchings to be the minimum of cardinalities of set V_1 and set V_2. Eq. (1) is a static optimization problem that minimizes total matching distances. It may suffer from matching vehicles with long-distance passengers. Also, it considers only the *current* location of the idle/transferred ride-sourcing vehicles and waiting passengers at *fixed* matching intervals. In Section 3.2, we consider the effect of the system's future state, i.e., the arrival of idle/transferred ride-sourcing vehicles and waiting passengers, congestion of the network, and the joint relationship of matching intervals and discarding long-distance matchings in the proposed method.

3.2. Adaptive spatio-temporal matching method

The adaptive spatio-temporal filtering method dynamically determines the maximum value for the matching distance between idle/transferred ride-sourcing vehicles and waiting passengers, as well as the occurrence time of the next matching. The maximum matching distance has immediate and future effects on vehicle–passenger matchings. A lower maximum matching distance leads to discarding more long-distance matchings from the solution of Eq. (1) to be discarded. Thus, it decreases the average distance of vehicle–passenger matchings at the cost of increasing the vehicles' and passengers' unassigned time. On the other hand, a higher maximum matching distance increases vehicles' and passengers' reserved time. When determining the occurrence of the next matching, a higher matching frequency (i.e., decreasing the time between two successive matching instances) reduces the number of idle/transferred vehicles and waiting passengers to be considered for matching. Consequently, the optimal myopic method would produce results with longer matching distances. In other words, a higher matching frequency decreases the *unassigned time* but increases the expected *reserved time*. Unassigned time for a ride-sourcing vehicle (passenger) is the time between the idle (waiting) state and dispatched (assigned) state. The reserved time for a ride-sourcing vehicle (passenger) is the time it takes for a dispatched vehicle (assigned passenger) to become occupied (on-board).

The adaptive spatio-temporal matching method aims to minimize the expected total passengers' waiting time (i.e., unassigned time plus the reserved time) by jointly determining the optimum time of the next matching instance and discarding the vehicle–passenger long-distance matchings. To this end, first, we use the optimal myopic vehicle–passenger matchings (i.e., considering the matching without discarding long-distance matchings) by solving Eq. (1). Subsequently, we define an expected passengers' waiting time based on the obtained values of the optimal myopic vehicle–passenger matchings. Then, we determine the optimum value of the next matching instance and the maximum distance for vehicle–passenger matchings to minimize the defined expected total passengers' waiting time. The expected total passengers' waiting time consists of four components: (i) *estimated* total reserved time, (ii) *estimated* total unassigned time, (iii) *predicted* total reserved time, and (iv) *predicted* total unassigned time. Fig. 3 illustrates the relationship among these components. To determine the above components, we assume that the average arrival rates of new waiting passengers and idle vehicles are known.

The expected total passengers' waiting time, $\hat{T}_{\mathrm{P}}^{t_{\mathrm{m}}^{t+1}-t_{\mathrm{m}}^{t}}$, between two successive matching time instances, t_{m}^{t} and t_{m}^{t+1}, is sum of four main parts:

(i) Estimated total reserved time of matchings at t_{m}^{t} is:

$$\hat{T}_{\mathrm{R}}(t_{\mathrm{m}}^{t}) = \frac{\bar{l}_r(t_{\mathrm{m}}^{t})}{\hat{v}(t_{\mathrm{m}}^{t})}\left(m(t_{\mathrm{m}}^{t}) - r(t_{\mathrm{m}}^{t})\right) = \frac{\bar{l}_r(t_{\mathrm{m}}^{t})}{\hat{v}(t_{\mathrm{m}}^{t})}\left(\min\left(c^{\mathrm{I}}(t_{\mathrm{m}}^{t}) + c^{\mathrm{T}}(t_{\mathrm{m}}^{t}), p^{\mathrm{W}}(t_{\mathrm{m}}^{t})\right) - r(t_{\mathrm{m}}^{t})\right), \tag{2}$$

where $\hat{T}_{\mathrm{R}}(t_{\mathrm{m}}^{t})$ is the estimated total reserved time for the idle/transferred vehicles assigned to the waiting passengers at t_{m}^{t}. The number of the matchings before discarding at time t_{m}^{t} is denoted by $m(t_{\mathrm{m}}^{t})$ from the solution of Eq. (1) at time instance t_{m}^{t}. $\bar{l}_r(t_{\mathrm{m}}^{t})$ is the average distance of optimum vehicle–passenger matchings after discarding $r(t_{\mathrm{m}}^{t})$ long-distance matchings. The number of idle vehicles, transfer vehicles, and waiting passengers at time t_{m}^{t} (before matching) are indicated by $c^{\mathrm{I}}(t_{\mathrm{m}}^{t})$, $c^{\mathrm{T}}(t_{\mathrm{m}}^{t})$, and $p^{\mathrm{W}}(t_{\mathrm{m}}^{t})$. $\hat{v}(t_{\mathrm{m}}^{t})$ denotes the estimated network speed at time instance t_{m}^{t}.

(ii) Estimated total unassigned time of the waiting passengers remaining in the network after the vehicle–passenger matching at t_{m}^{t} with discarding $r(t_{\mathrm{m}}^{t})$ long-distance matching, $\hat{T}_{\mathrm{D}}(t_{\mathrm{m}}^{t})$, is:

$$\hat{T}_{\mathrm{D}}(t_{\mathrm{m}}^{t}) = \left(p^{\mathrm{W}}(t_{\mathrm{m}}^{t}) - m(t_{\mathrm{m}}^{t}) + r(t_{\mathrm{m}}^{t})\right)\left(t_{\mathrm{m}}^{t+1} - t_{\mathrm{m}}^{t}\right). \tag{3}$$

(iii) Predicted total reserved time for matchings at t_{m}^{t+1}, $\hat{T}_{\mathrm{R}}(t_{\mathrm{m}}^{t+1})$, is:

$$\begin{aligned}\hat{T}_{\mathrm{R}}(t_{\mathrm{m}}^{t+1}) &= \frac{\hat{\bar{l}}_r(t_{\mathrm{m}}^{t+1})}{\hat{v}(t_{\mathrm{m}}^{t+1})}\left(m(t_{\mathrm{m}}^{t+1}) + r(t_{\mathrm{m}}^{t})\right)\\ &= \frac{\hat{\bar{l}}_r(t_{\mathrm{m}}^{t+1})}{\hat{v}(t_{\mathrm{m}}^{t})}\left(\min\left(c^{\mathrm{I}}(t_{\mathrm{m}}^{t}) + c^{\mathrm{T}}(t_{\mathrm{m}}^{t}) + \rho_{\mathrm{c}}(t_{\mathrm{m}}^{t})\left(t_{\mathrm{m}}^{t+1} - t_{\mathrm{m}}^{t}\right) - m(t_{\mathrm{m}}^{t}), p^{\mathrm{W}}(t_{\mathrm{m}}^{t}) + \rho_{\mathrm{p}}(t_{\mathrm{m}}^{t})\left(t_{\mathrm{m}}^{t+1} - t_{\mathrm{m}}^{t}\right) - m(t_{\mathrm{m}}^{t})\right) + r(t_{\mathrm{m}}^{t})\right),\end{aligned} \tag{4}$$

with

$$\rho_{\mathrm{c}}(t_{\mathrm{m}}^{t}) = \rho_{\mathrm{c}}^{\mathrm{en}}(t_{\mathrm{m}}^{t}) + \rho_{\mathrm{c}}^{\mathrm{ex}}(t_{\mathrm{m}}^{t}),$$

where $\hat{\bar{l}}_r(t_{\mathrm{m}}^{t+1})$ estimates the average matching distance of matched pairs in a bipartite matching program as Eq. (1). This parameter is defined to predict the average matching distance in the next matching instance, t_{m}^{t+1}, not reflecting the current (at t_{m}^{t}) observed value ($\bar{l}_r(t_{\mathrm{m}}^{t})$). Since the exact locations of idle/transferred vehicles and waiting passengers at time t_{m}^{t+1} are not known, we propose a parsimonious function to estimate the average matching distance of the optimum matching that is only a function of the number of vehicles and passengers. Section 3.3 explains estimation of $\hat{\bar{l}}_r(t_{\mathrm{m}}^{t+1})$. $m(t_{\mathrm{m}}^{t+1})$ denotes the number of matchings at time t_{m}^{t+1} without discarding at time t_{m}^{t}. The rates of arrival of idle/transferred vehicles and waiting passengers during interval $[t_{\mathrm{m}}^{t}, t_{\mathrm{m}}^{t+1})$ are denoted by $\rho_{\mathrm{c}}(t_{\mathrm{m}}^{t})$ and $\rho_{\mathrm{p}}(t_{\mathrm{m}}^{t})$, respectively. $\rho_{\mathrm{c}}(t_{\mathrm{m}}^{t})$ consists of endogenous, $\rho_{\mathrm{c}}^{\mathrm{en}}(t_{\mathrm{m}}^{t})$, and exogenous parts, $\rho_{\mathrm{c}}^{\mathrm{ex}}(t_{\mathrm{m}}^{t})$. $\rho_{\mathrm{c}}^{\mathrm{en}}(t_{\mathrm{m}}^{t})$ captures the rate that occupied or dispatched vehicles become idle. $\rho_{\mathrm{c}}^{\mathrm{ex}}(t_{\mathrm{m}}^{t})$ captures the rate of idle ride-sourcing vehicles leaving from or entering into the network.

(iv) Predicted total unassigned time for waiting passengers remaining in the network after the vehicle–passenger matching at t_{m}^{t+1}, $\hat{T}_{\mathrm{D}}(t_{\mathrm{m}}^{t+1})$, is:

$$\begin{aligned}\hat{T}_{\mathrm{D}}(t_{\mathrm{m}}^{t+1}) &= \left(p^{\mathrm{W}}(t_{\mathrm{m}}^{t}) + \rho_{\mathrm{p}}(t_{\mathrm{m}}^{t})\left(t_{\mathrm{m}}^{t+1} - t_{\mathrm{m}}^{t}\right) - \left(m(t_{\mathrm{m}}^{t}) - r(t_{\mathrm{m}}^{t})\right) - \left(m(t_{\mathrm{m}}^{t+1}) + r(t_{\mathrm{m}}^{t})\right)\right) \times \left(t_{\mathrm{m}}^{t+2} - t_{\mathrm{m}}^{t+1}\right)\\ &= \left(p^{\mathrm{W}}(t_{\mathrm{m}}^{t}) + \rho_{\mathrm{p}}(t_{\mathrm{m}}^{t})\left(t_{\mathrm{m}}^{t+1} - t_{\mathrm{m}}^{t}\right) - m(t_{\mathrm{m}}^{t}) - m(t_{\mathrm{m}}^{t+1})\right)\left(t_{\mathrm{m}}^{t+2} - t_{\mathrm{m}}^{t+1}\right).\end{aligned} \tag{5}$$

In Eq. (5), we assume the discarded matchings at time t_{m}^{t}, i.e., $r(t_{\mathrm{m}}^{t})$, will be matched at time t_{m}^{t+1}.

Thus, the expected total passengers' waiting time is[2]:

$$\hat{T}_{\mathrm{P}}^{t_{\mathrm{m}}^{t+1}-t_{\mathrm{m}}^{t}} = \hat{T}_{\mathrm{R}}(t_{\mathrm{m}}^{t}) + \hat{T}_{\mathrm{D}}(t_{\mathrm{m}}^{t}) + \hat{T}_{\mathrm{R}}(t_{\mathrm{m}}^{t+1}) + \hat{T}_{\mathrm{D}}(t_{\mathrm{m}}^{t+1}). \tag{6}$$

[2] Note that a term representing predicted waiting time of passengers arriving between t_{m}^{t} and t_{m}^{t+1}, is not considered in Eq. (6). If the exogenous arrival rate of passengers, $\rho_p(t_{\mathrm{m}}^{t})$, is assumed to be spread uniformly between t_{m}^{t} and t_{m}^{t+1}, then the predicted waiting time of passengers arriving between t_{m}^{t} and t_{m}^{t+1} would read as $0.5\rho_p(t_{\mathrm{m}}^{t})(t_{\mathrm{m}}^{t+1} - t_{\mathrm{m}}^{t})^2$. If one assumes the exogenous arrival rate of passengers, $\rho_p(t_{\mathrm{m}}^{t})$, appears at the end of the interval (i.e., t_{m}^{t+1}), then the predicted waiting time of passengers arriving between t_{m}^{t} and t_{m}^{t+1} would be zero. Nevertheless, the relative value of this term compared to the other four terms in the objective function (6) is minor. It is expected that considering this term will result in insignificant changes in the numerical results if a uniform arrival formulation is used instead of an end-loaded arrival calculation.

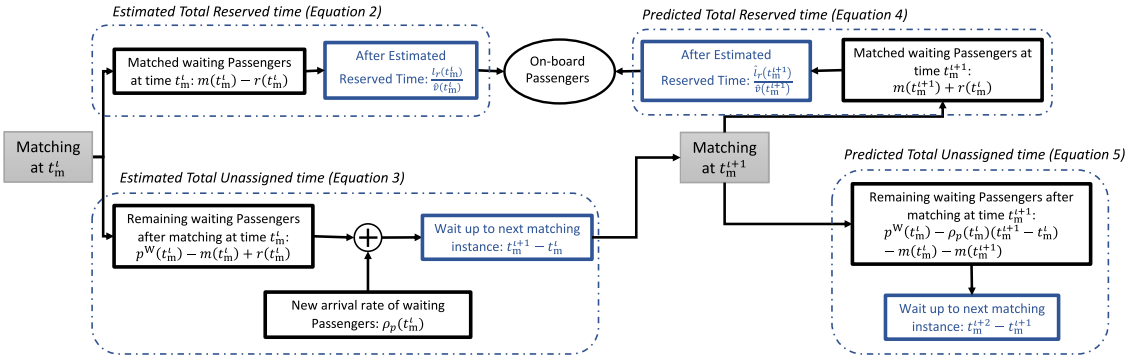

Fig. 3. Schematic of relation among estimated total reserved time (Eq. (2)), estimated total unassigned time (Eq. (3)), predicted total reserved time (Eq. (4)), and predicted total unassigned time (Eq. (5)). Blue boxes represent the time components and black boxes illustrate passengers.

We obtain the optimum value for the next two matching times, $t^{\iota+1}_{\mathrm{m}}$ and $t^{\iota+2}_{\mathrm{m}}$, and the number of discarded long-distance matchings, $r(t^{\iota}_{\mathrm{m}})$, by minimizing the total passengers' waiting time prediction as determined in Eq. (7).

$$\begin{aligned} &\underset{r(t^{\iota}_{\mathrm{m}}),t^{\iota+1}_{\mathrm{m}},t^{\iota+2}_{\mathrm{m}}}{\text{minimize}} \quad \left(\hat{T}_{\mathrm{P}}^{t^{\iota+1}_{\mathrm{m}}-t^{\iota}_{\mathrm{m}}}\right) \\ &\text{s.t.} \quad 0 < t^{\iota}_{\mathrm{m}} < t^{\iota+1}_{\mathrm{m}} \le t^{\iota+2}_{\mathrm{m}} \le t^{\iota}_{\mathrm{m}} + t^{\max}_{\mathrm{m}}, \quad 0 \le r(t^{\iota}_{\mathrm{m}}) \le m(t^{\iota}_{\mathrm{m}}), \end{aligned} \tag{7}$$

where $t^{\max}_{\mathrm{m}}$ is a predefined upper bound for the next matching time instance.

One can verify that $t^{\iota+2}_{\mathrm{m}}$ only appears in Eq. (5), in which an intuitive solution to the minimization program of Eq. (7) would be $t^{\iota+1}_{\mathrm{m}} = t^{\iota+2}_{\mathrm{m}}$. Hence, Eq. (7) can be reformulated as below to obtain the optimum value for the next matching time, $t^{\iota+1}_{\mathrm{m}}$, and the number of discarded long-distance matchings, $r(t^{\iota}_{\mathrm{m}})$:

$$\begin{aligned} &\underset{r(t^{\iota}_{\mathrm{m}}),t^{\iota+1}_{\mathrm{m}}}{\text{minimize}} \quad \left(\hat{T}_{\mathrm{P}}^{t^{\iota+1}_{\mathrm{m}}-t^{\iota}_{\mathrm{m}}}\right) \\ &\text{s.t.} \quad 0 < t^{\iota}_{\mathrm{m}} < t^{\iota+1}_{\mathrm{m}} \le t^{\iota}_{\mathrm{m}} + t^{\max}_{\mathrm{m}}, \quad 0 \le r(t^{\iota}_{\mathrm{m}}) \le m(t^{\iota}_{\mathrm{m}}). \end{aligned} \tag{8}$$

To practically solve the discrete–continuous optimization problem of Eq. (8), after solving the optimal myopic matching program, we discretize the time domain, $[t^{\iota}_{\mathrm{m}}, t^{\iota}_{\mathrm{m}} + t^{\max}_{\mathrm{m}}]$, and iteratively evaluate Equation 6 for any specific $t^{\iota+1}_{\mathrm{m}}$ and $r(t^{\iota}_{\mathrm{m}})$ that satisfies the criteria of Eq. (8) to determine the optimum values. Choosing $t^{\max}_{\mathrm{m}}$ and sampling period for discretization are crucial factors to reach an attainable solution computationally. We choose $t^{\max}_{\mathrm{m}} = 120\,[\mathrm{s}]$ and sampling period of $2\,[\mathrm{s}]$.

The major time complexity of solving the optimization problem is stemmed from solving the optimal myopic matchings that can be relaxed significantly from $O((\|V_1\| + \|V_2\|)^4)$ to $O(\sqrt{\|V_1\| + \|V_2\|})$ by adopting an approximate method instead of an exact method (Vazirani, 1994). Recall that V_1 is the set of idle and transferred vehicles, V_2 is the set of waiting passengers, and $\|V_1\|$ denotes the size of set V_1. The performance of the proposed adaptive spatio-temporal matching method for dispatching idle/transferred vehicles to waiting passengers is investigated in Section 5.

3.3. Estimating a macro-function for average optimal myopic matching distance

A closed-form macro-function for estimating average optimal myopic matching distance, $\hat{\bar{l}}$, is needed for predicting the total reserved time, see Eq. (4). To this end, we propose Algorithm 1 (as a proxy) to estimate the average optimal myopic matching distance as a function of the number of idle/transferred ride-sourcing vehicles and waiting passengers, independent of their location. Algorithm 1 generates the locations of idle/transferred ride-sourcing vehicles and waiting passengers randomly with uniform distribution inside a network. Then, a bipartite graph, $G(V_1, V_2, E)$, is built in which the weights of the edges are the Manhattan distance between idle/transferred ride-sourcing vehicles and waiting passengers. The average optimal matching is determined by solving the matching problem on graph G minimizing the sum of matching weights as in Eq. (1). To tackle the stochasticity of the spatial distribution of ride-sourcing vehicles and passengers, this procedure is repeated N^{itr} times for each number of idle/transferred ride-sourcing vehicles and waiting passengers. This experiment is conducted for a range of passengers, 1 to N^{P}, and a range of vehicles, 1 to N^{T}, where N^{P} and N^{T} denote the maximum numbers of passengers and vehicles that are considered, respectively.

We run the algorithm on a high-performance computer (HPC) for N^{itr}=100, N^{P}=50, and N^{T}=50. The result, see Fig. 4(b), reveals that the variations of average optimum matching distance with respect to the number of waiting passengers and idle/transferred ride-sourcing vehicles are:

$$\begin{cases} \frac{\partial \hat{\bar{l}}}{\partial (c^{\mathrm{I}}+c^{\mathrm{T}})} > 0, \ \frac{\partial \hat{\bar{l}}}{\partial p^{\mathrm{W}}} < 0 & \text{if } c^{\mathrm{I}} + c^{\mathrm{T}} < p^{\mathrm{W}} \\ \frac{\partial \hat{\bar{l}}}{\partial (c^{\mathrm{I}}+c^{\mathrm{T}})} < 0, \ \frac{\partial \hat{\bar{l}}}{\partial p^{\mathrm{W}}} > 0 & \text{if } p^{\mathrm{W}} < c^{\mathrm{I}} + c^{\mathrm{T}} \end{cases}$$

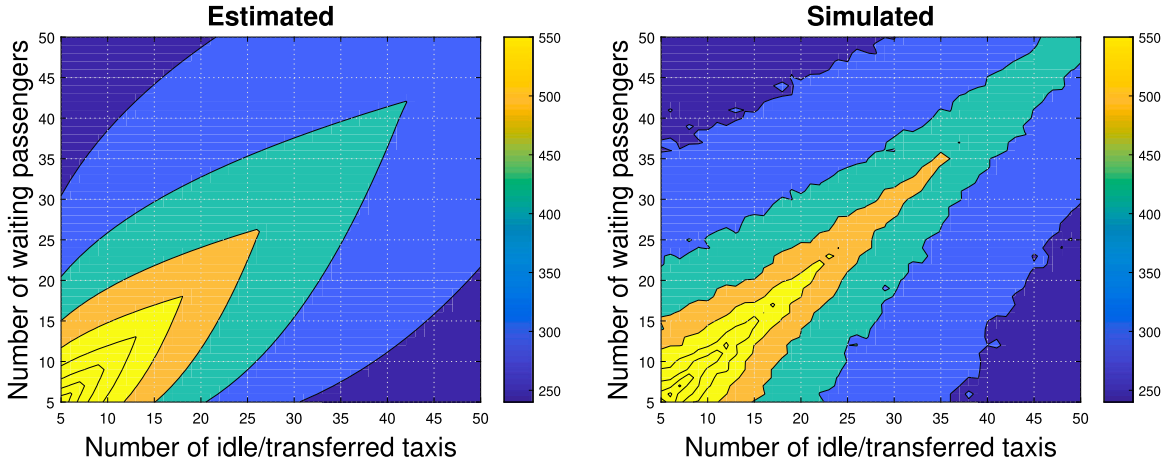

Fig. 4. (a) Estimated average of optimum matching distance [m] and (b) simulated average of optimum matching distance [m].

Accordingly, the following symmetric function is suggested to estimate the average optimum matching distance:

$$\hat{\bar{l}} = \begin{cases} \theta(c^{\mathrm{I}} + c^{\mathrm{T}})^{\zeta_1} p^{\mathrm{W}\zeta_2} & \text{if} \quad c^{\mathrm{I}} + c^{\mathrm{T}} \le p^{\mathrm{W}} \\ \theta(c^{\mathrm{I}} + c^{\mathrm{T}})^{\zeta_2} p^{\mathrm{W}\zeta_1} & \text{if} \quad p^{\mathrm{W}} < c^{\mathrm{I}} + c^{\mathrm{T}} \end{cases} \tag{9}$$

where $\theta > 0$, $\zeta_1 > 0$, and $\zeta_2 < 0$ are parameters that can be readily estimated using the Least Square method. By utilizing the generated data in Algorithm 1, the estimated values of the parameters are: $\hat{\theta} = 2394.57$, $\hat{\zeta_1} = 0.245$, and $\hat{\zeta_2} = -0.724$, where $R^2 = 0.93$. Fig. 4 compares the simulated and estimated average optimum matching distances.

Algorithm 1: Pseudocode for estimating the average optimum matching distance

Result: $\{\hat{\bar{l}}_{n^{\mathrm{P}} \times n^{\mathrm{T}}} |\ n^{\mathrm{P}} = 1 : N^{\mathrm{P}},\ n^{\mathrm{T}} = 1 : N^{\mathrm{T}}\}$
Spatial initialization;
for $n^{\mathrm{T}} = 1 : N^{\mathrm{T}}$ **do**
  for $n^{\mathrm{P}} = 1 : N^{\mathrm{P}}$ **do**
    for $k = 1 : N^{\mathrm{itr}}$ **do**
      $\{(x_i^{\mathrm{P}}, y_i^{\mathrm{P}}) |\ i = 1 : n^{\mathrm{P}}\} \leftarrow$ Generate coordinates of n^{P} passengers randomly;
      $\{(x_j^{\mathrm{T}}, y_j^{\mathrm{T}}) |\ j = 1 : n^{\mathrm{T}}\} \leftarrow$ Generate coordinates of n^{T} ride-sourcing vehicles randomly;
      $G(V_1, V_2, E) \leftarrow$ Initialization a bipartite graph with $|V_1| = n^{\mathrm{P}}$ and $|V_2| = n^{\mathrm{T}}$;
      for $i = 1 : n^{\mathrm{P}}$ **do**
        for $j = 1 : n^{\mathrm{T}}$ **do**
          $w_{ij} \leftarrow$ Manhattan distance between passenger i and ride-sourcing vehicle j;
          $d_{ij} \leftarrow$ Add an edge to connect vertices $(v_1^{\mathrm{i}}, v_2^{\mathrm{j}})$ with weight w_{ij};
      $M_k \leftarrow$ Find optimal matching of G to minimize the sum of matching weights;
      $\hat{l}_k \leftarrow$ Find the average of matched weights;
    $\hat{\bar{l}}_{n^{\mathrm{P}} \times n^{\mathrm{T}}} \leftarrow$ Find the average of $\{\hat{l}_k |\ k = 1 : N^{\mathrm{itr}}\}$;

4. Model formulation

Consider a network divided into a set of $\mathbb{R}$ regions. The proposed ride-sourcing model formulates the interaction of waiting passengers, assigned passengers, idle ride-sourcing vehicles, occupied ride-sourcing vehicles, dispatched ride-sourcing vehicles, and transferred ride-sourcing vehicles in different regions as illustrated in the state diagrams of Fig. 1. We develop the model based on MFD and Cobb–Douglas meeting function. The ride-sourcing model is a set of first-order differential equations representing mass conservation dynamics of the ride-sourcing vehicles and passengers.

MFD is a macroscopic relationship between the number of vehicles (accumulation) and aggregated outflow (or weighted flow of links, production) in homogeneous regions. The existence of this relationship is empirically presented in Geroliminis and Daganzo (2008). The effect of congestion heterogeneity on MFD properties is studied in Mahmassani et al. (2013) and Ramezani et al. (2015). A three-step clustering algorithm is proposed in Saeedmanesh and Geroliminis (2016) to partition heterogeneous networks into a few connected homogeneous regions. This offers traffic management opportunities based on MFD modeling such as perimeter

control (Li et al., 2021; Haddad and Zheng, 2020), regional routing (Ingole et al., 2020), and regional pricing (Zheng et al., 2012), among others. The applicability of MFD in modeling of on-demand mobility services including cruising taxi systems, ride-sharing systems, and pricing of ride-sourcing systems, are studied in Ramezani and Nourinejad (2018), Nourinejad and Ramezani (2019), Alisoltani et al. (2021) and Beojone and Geroliminis (2021).

In this paper, the MFD is used to estimate the internal and inter-regional flows[3] of occupied and transferred ride-sourcing vehicles as well as the inter-regional flow of the dispatched ride-sourcing vehicles. Cobb–Douglas meeting functions are utilized to model the boarding rate of assigned passengers and the rate at which dispatched ride-sourcing vehicles become occupied. The reason for differentiating between estimating the internal flow of dispatched ride-sourcing vehicles and occupied/transferred ride-sourcing vehicles is their travel behaviors. The average trip length for the internal flow of the dispatched ride-sourcing vehicles is highly sensitive to the number of the dispatched ride-sourcing vehicles and assigned passengers. Assuming that the number of the dispatched ride-sourcing vehicles is constant, the higher the number of assigned passengers, the lower the average trip length is. Hence, we use Cobb–Douglas meeting function to estimate the boarding rate within the region, which allows us to infer the number of dispatched ride-sourcing vehicles and assigned passengers simultaneously. However, the average trip lengths for the occupied/transferred ride-sourcing vehicles as well as the inter-regional dispatched ride-sourcing vehicles are independent of the number of passengers. That is, their travel patterns are similar to the normal vehicles. Therefore, we utilize MFDs to estimate their trip completions.

The boarding function between dispatched ride-sourcing vehicles and assigned passengers in Region i, b_i, is defined by a Cobb–Douglas type meeting function to consider the friction and congestion (Yang and Yang, 2011; Ramezani and Nourinejad, 2018):

$$\begin{aligned} b_i(t) &= K_i c_{ii}^{\mathrm{D}}(t)^{\alpha_i} p_i^{\mathrm{A}}(t)^{\beta_i} v_i(t)^{\gamma_i} \qquad \forall i \in \mathbb{R}, \\ p_i^{\mathrm{A}}(t) &= \sum_{j \in \{\mathbb{U}_i \cup i\}} p_{ij}^{\mathrm{A}}(t) \qquad \forall i \in \mathbb{R}, \end{aligned} \tag{10}$$

where K_i is the total productivity factor of Region i. The number of dispatched ride-sourcing vehicles in Region i with pickup location in Region i at time t is denoted by $c_{ii}^{\mathrm{D}}(t)$. The total number of assigned passengers in Region i and the number of assigned passengers in Region i with destinations in Region j are denoted by $p_i^{\mathrm{A}}(t)$ and $p_{ij}^{\mathrm{A}}(t)$, respectively. $\mathbb{U}_i$ is the set of regions in the direct vicinity of Region i. $v_i(t)$ is the average speed in Region i. Note that the average speed is considered in the boarding function to reflect the effect of congestion on the meeting rate (Ramezani and Nourinejad, 2018). The elasticities with respect to the number of dispatched vehicles, assigned passengers, and average speed are denoted by α_i, β_i, and γ_i, respectively. K_i, α_i, β_i, and γ_i are constant parameters that can be estimated from the field or simulated data.

By defining the total boarding rate in Region i as Eq. (10), the boarding rate in Region i with the final destination in Region j at time t can be approximated from the following equation (assuming the boarding rate is proportional to assigned passengers):

$$b_{ij}(t) = \frac{p_{ij}^{\mathrm{A}}(t)}{p_i^{\mathrm{A}}(t)} b_i(t) \qquad \forall i \in \mathbb{R} \ \text{ and } \ j \in \{\mathbb{U}_i, i\} \ . \tag{11}$$

We use the production MFD to obtain the inter-regional flows of occupied vehicles, $M_{ij}^{\mathrm{O}}(t)$, transferred vehicles, $M_{ij}^{\mathrm{T}}(t)$, and dispatched vehicles, $M_{ij}^{\mathrm{D}}(t)$. We assume the inter-regional flows are proportional to the corresponding accumulations:

$$M_{ij}^{\mathrm{O}}(t) = \frac{c_{ij}^{\mathrm{O}}(t)}{n_i(t)} \frac{P_i(n_i(t))}{l_{ij}^{\mathrm{O}}(t)} \qquad \forall i \in \mathbb{R} \ \text{ and } \ j \in \mathbb{U}_i \ , \tag{12}$$

$$M_{ij}^{\mathrm{T}}(t) = \frac{c_{ij}^{\mathrm{T}}(t)}{n_i(t)} \frac{P_i(n_i(t))}{l_{ij}^{\mathrm{T}}(t)} \qquad \forall i \in \mathbb{R} \ \text{ and } \ j \in \mathbb{U}_i \ , \tag{13}$$

$$M_{ij}^{\mathrm{D}}(t) = \frac{c_{ij}^{\mathrm{D}}(t)}{n_i(t)} \frac{P_i(n_i(t))}{l_{ij}^{\mathrm{D}}(t)} \qquad \forall i \in \mathbb{R} \ \text{ and } \ j \in \mathbb{U}_i \ , \tag{14}$$

where $c_{ij}^{\mathrm{O}}(t)$, $c_{ij}^{\mathrm{T}}(t)$, and $c_{ij}^{\mathrm{D}}(t)$ are respectively the number of the occupied, transferred, and dispatched vehicles in Region i moving to Region j at time t. $n_i(t)$ is the total accumulation of vehicles in Region i including normal vehicles and all types of ride-sourcing vehicles in Region i. $P_i(n_i(t))$ is the production MFD in Region i that is a function of the total accumulation in Region i. The average trip length for occupied, transferred, and dispatched vehicles in Region i that travel to Region j are denoted by $l_{ij}^{\mathrm{O}}(t)$, $l_{ij}^{\mathrm{T}}(t)$, and $l_{ij}^{\mathrm{D}}(t)$, respectively.

The internal flows for the occupied, $M_{ii}^{\mathrm{O}}(t)$, and the transferred ride-sourcing vehicles, $M_{ii}^{\mathrm{T}}(t)$, are:

$$M_{ii}^{\mathrm{O}}(t) = \frac{c_{ii}^{\mathrm{O}}(t)}{n_i(t)} \frac{P_i(n_i(t))}{l_{ii}^{\mathrm{O}}(t)} \qquad \forall i \in \mathbb{R}, \tag{15}$$

$$M_{ii}^{\mathrm{T}}(t) = \frac{c_{ii}^{\mathrm{T}}(t)}{n_i(t)} \frac{P_i(n_i(t))}{l_{ii}^{\mathrm{T}}(t)} \qquad \forall i \in \mathbb{R}, \tag{16}$$

[3] In MFD literature, this term is typically named transfer flow. However, to avoid confusion with the transfer state of ride-sourcing vehicles, we use the inter-region flow term in this paper.

where $c_{ii}^{\mathrm{O}}(t)$ and $c_{ii}^{\mathrm{T}}(t)$ are the number of occupied and transferred ride-sourcing vehicles in Region i with destination in Region i. $l_{ii}^{\mathrm{O}}(t)$ and $l_{ii}^{\mathrm{T}}(t)$ denote the average trip length of occupied and transferred vehicles in Region i with destinations in Region i.

Using the above internal and inter-regional flows, we can derive the dynamics of different system states as mass conservation formulations. The conservation of the number of occupied ride-sourcing vehicles is modeled as:

$$\frac{\mathrm{d}c_{ii}^{\mathrm{O}}(t)}{\mathrm{d}t} = b_{ii}(t) + \sum_{j\in\mathbb{U}_i} M_{ji}^{\mathrm{O}}(t) - M_{ii}^{\mathrm{O}}(t) \qquad \forall i \in \mathbb{R}, \tag{17}$$

$$\frac{\mathrm{d}c_{ij}^{\mathrm{O}}(t)}{\mathrm{d}t} = b_{ij}(t) - M_{ij}^{\mathrm{O}}(t) \qquad \forall i \in \mathbb{R} \ \text{ and } \ j \in \mathbb{U}_i. \tag{18}$$

In RHS of Eqs. (17) and (18), $b_{ii}(t)$ and $b_{ij}(t)$ are the number of the dispatched ride-sourcing vehicles that become occupied with destinations in Regions i and j respectively. $\sum_{j\in\mathbb{U}_i} M_{ji}^{\mathrm{O}}(t)$ reflects the rate at which occupied ride-sourcing vehicles from regions in $\mathbb{U}_i$ cross the regional boundary towards Region i. $M_{ii}^{\mathrm{O}}(t)$ is the rate that occupied ride-sourcing vehicles within Region i complete their trips and become idle.

The evolution of the number of dispatched ride-sourcing vehicles over time is:

$$\frac{\mathrm{d}c_{ii}^{\mathrm{D}}(t)}{\mathrm{d}t} = W_{ii}^{\text{I-D}}(t) + W_{ii}^{\text{T-D}}(t) + \sum_{j\in\mathbb{U}_i} M_{ji}^{\mathrm{D}}(t) - b_i(t) - R_{ii}^{\mathrm{D}}(t) \qquad \forall i \in \mathbb{R}, \tag{19}$$

$$\frac{\mathrm{d}c_{ij}^{\mathrm{D}}(t)}{\mathrm{d}t} = W_{ij}^{\text{I-D}}(t) + W_{ij}^{\text{T-D}}(t) - M_{ij}^{\mathrm{D}}(t) - R_{ij}^{\mathrm{D}}(t) \qquad \forall i \in \mathbb{R} \ \text{ and } \ j \in \mathbb{U}_i, \tag{20}$$

where c_{ii}^{D} and c_{ij}^{D} respectively denote the number of the dispatched ride-sourcing vehicles in Region i with pickup location in Regions i and j. $W_{ii}^{\text{I-D}}(t)$ and $W_{ij}^{\text{I-D}}(t)$ are the rates at which the matching method dispatches idle ride-sourcing vehicles in Region i to Regions i and j at time t, respectively. $W_{ii}^{\text{T-D}}(t)$ and $W_{ij}^{\text{T-D}}(t)$ denote the rates that the matching method dispatches transferred ride-sourcing vehicles in Region i to Regions i and j at time t. Variables $W_{ii}^{\text{I-D}}(t)$, $W_{ij}^{\text{I-D}}(t)$, $W_{ii}^{\text{T-D}}(t)$, and $W_{ij}^{\text{T-D}}(t)$ are the solution of the dispatching subsystem (see Fig. 2) at each matching time instance. $R_{ii}^{\mathrm{D}}(t)$ and $R_{ij}^{\mathrm{D}}(t)$ are the cancellation rate of dispatched trips at time t in Region i with final destinations (i.e., pickup locations) in Regions i and j, respectively. They represent the cancellation of dispatched trips before and after crossing the boundary. For example, consider a ride-sourcing vehicle currently in Region 1 with the final dispatching destination in neighboring Region 4. If the trip is canceled at time t before crossing the boundary, it will be considered in $R_{14}^{\mathrm{D}}(t)$. Once the ride-sourcing vehicle crosses the boundary and the trip gets canceled, it will be considered in $R_{44}^{\mathrm{D}}(t)$.

The number of the transferred ride-sourcing vehicles at each time is obtained from the following equations. We assume that the transferred ride-sourcing vehicles in Region i complete their trips within Region i:

$$\frac{\mathrm{d}c_{ii}^{\mathrm{T}}(t)}{\mathrm{d}t} = \sum_{j\in\mathbb{U}_i} M_{ji}^{\mathrm{T}}(t) - M_{ii}^{\mathrm{T}}(t) - W_{ii}^{\text{T-D}}(t) \qquad \forall i \in \mathbb{R}, \tag{21}$$

$$\frac{\mathrm{d}c_{ij}^{\mathrm{T}}(t)}{\mathrm{d}t} = W_{ij}^{\text{I-T}}(t) - M_{ij}^{\mathrm{T}}(t) - W_{ij}^{\text{T-D}}(t) \qquad \forall i \in \mathbb{R} \ \text{ and } \ j \in \mathbb{U}_i, \tag{22}$$

where $W_{ij}^{\text{I-T}}(t)$ is the rate that idle vehicles in Region i are advised to transfer to Region j by the transfer controller. This external manipulating (i.e., control) variable is obtained from the transfer subsystem to balance the number of idle ride-sourcing vehicles and waiting passengers in the network. We propose a predictive controller in Part II to dynamically determine the optimum values of $W_{ij}^{\text{I-T}}(t)$.

The total number of idle ride-sourcing vehicles in Region i is evolved based on the following equation:

$$\frac{\mathrm{d}c_{i}^{\mathrm{I}}(t)}{\mathrm{d}t} = q_i^{c^+}(t) + M_{ii}^{\mathrm{O}}(t) + M_{ii}^{\mathrm{T}}(t) - q_i^{c^-}(t) + \sum_{j\in\{\mathbb{U}_i,i\}} R_{ij}^{\mathrm{D}}(t) - \sum_{j\in\{\mathbb{U}_i,i\}} W_{ij}^{\text{I-D}}(t) - \sum_{j\in\mathbb{U}_i} W_{ij}^{\text{I-T}}(t) + w_i^{\mathrm{I}}(t) \quad \forall i \in \mathbb{R}, \tag{23}$$

where $q_i^{c^+}(t)$ is the rate of idle ride-sourcing vehicles exogenously enter to the network at time t. $q_i^{c^-}(t)$ denotes the rate of idle ride-sourcing vehicles leaving the network at time t because of finishing their working hours. $M_{ii}^{\mathrm{O}}(t)$ and $M_{ii}^{\mathrm{T}}(t)$ reflect the rate of occupied and transferred ride-sourcing vehicles completing their trips and becoming idle. The total number of the idle ride-sourcing vehicles becoming dispatched and transferred in Region i are considered in $\sum_{j\in\mathbb{U}_i} W_{ij}^{\text{I-D}}(t)$ and $\sum_{j\in\mathbb{U}_i} W_{ij}^{\text{I-T}}(t)$ terms. Some idle ride-sourcing vehicles prefer to park or cruise until they are dispatched to an assigned passenger. $w_i^{\mathrm{I}}(t)$ is a stochastic term that represents the rate that idle vehicles enter (or leave) Region i at time t because of their random cruising; this might happen to non-dispatched non-transferred idle vehicles that cruise around the boundary of regions. Intuitively, $\sum_{i\in\mathbb{R}}(q_i^{c^+}(t) - q_i^{c^-}(t)) = \rho_{\mathrm{c}}^{\mathrm{ex}}(t)$, which is the (exogenous) rate that idle ride-sourcing vehicles leave from or enter into the network (see Eq. (4)). Moreover, $\sum_{i\in\mathbb{R}} M_{ii}^{\mathrm{O}}(t) + \sum_{i\in\mathbb{R}}\sum_{j\in\{\mathbb{U}_i,i\}} R_{ij}^{\mathrm{D}}(t) = \rho_{\mathrm{c}}^{\mathrm{en}}(t)$, which is the (endogenous) rate that occupied or dispatched vehicles become idle (see Eq. (4)).

Based on Fig. 1, there are three states for the passengers in the proposed ride-sourcing system: (i) waiting passengers, (ii) assigned passengers, and (iii) on-board passengers. The conservation of the on-board passengers over time is exactly similar to the occupied ride-sourcing vehicles. However, we need to formulate the conservation of the number of waiting and assigned passengers. The following equations describe the dynamics of the waiting passengers:

$$\frac{\mathrm{d}p_{ii}^{\mathrm{W}}(t)}{\mathrm{d}t} = q_{ii}^{p^{W+}}(t) - q_{ii}^{p^{W-}}(t) - W_{ii}^{\text{W-A}}(t) \qquad \forall i \in \mathbb{R}, \tag{24}$$

$$\frac{\mathrm{d}p_{ij}^{\mathrm{W}}(t)}{\mathrm{d}t} = q_{ij}^{p^{W+}}(t) - q_{ij}^{p^{W-}}(t) - W_{ij}^{\text{W-A}}(t) \qquad \forall i \in \mathbb{R} \text{ and } j \in \mathbb{U}_i, \tag{25}$$

where $p_{ii}^{\mathrm{W}}(t)$ and $p_{ij}^{\mathrm{W}}(t)$ denote the number of waiting passengers in Region i with destinations in Region i and Region j at time t, respectively. The exogenous rate of waiting passenger demand in Region i traveling to Regions i and j are denoted by $q_{ii}^{p^{W+}}(t)$ and $q_{ij}^{p^{W+}}(t)$, respectively. $q_{ii}^{p^{W-}}(t)$ and $q_{ij}^{p^{W-}}(t)$ are the rate that waiting passengers in Region i with destination in Regions i and j leave the network at time t because of their dissatisfaction with the ride-sourcing system. Intuitively, $\sum_{i\in\mathbb{R}}(q_{ii}^{p^{W+}}(t) - q_{ii}^{p^{W-}}(t)) + \sum_{i\in\mathbb{R}}\sum_{j\in\mathbb{U}_i}(q_{ij}^{p^{W+}}(t) - q_{ij}^{p^{W-}}(t)) = \rho_{\mathrm{p}}(t)$, which is the rate of arrival of waiting passengers into the network (see Eq. (4)). The rate at which the waiting passengers in Region i with destinations in i and j become assigned at time t are denoted by $W_{ii}^{\text{W-A}}(t)$ and $W_{ij}^{\text{W-A}}(t)$, respectively. Parameters $W_{ii}^{\text{W-A}}(t)$ and $W_{ij}^{\text{W-A}}(t)$ are the outputs of the dispatching subsystem.

Finally, the number of assigned passengers is:

$$\frac{\mathrm{d}p_{ii}^{\mathrm{A}}(t)}{\mathrm{d}t} = W_{ii}^{\text{W-A}}(t) - q_{ii}^{p^{A-}}(t) - b_{ii}(t) \qquad \forall i \in \mathbb{R}, \tag{26}$$

$$\frac{\mathrm{d}p_{ij}^{\mathrm{A}}(t)}{\mathrm{d}t} = W_{ij}^{\text{W-A}}(t) - q_{ij}^{p^{A-}}(t) - b_{ij}(t) \qquad \forall i \in \mathbb{R} \text{ and } j \in \mathbb{U}_i, \tag{27}$$

where $q_{ii}^{p^{A-}}(t)$ and $q_{ij}^{p^{A-}}(t)$ are the rate of impatient assigned passengers in Region i with trip destinations in Regions i and j canceling their trips. The patience thresholds of passengers are set exogenously as stochastic parameters. $q_{ii}^{p^{A-}}(t)$ and $q_{ij}^{p^{A-}}(t)$ are endogenous parameters that reflect one quality aspect of the dispatching and transfer subsystems. Effective dispatching and transfer subsystems result in lower values of $q_{ii}^{p^{A-}}(t)$ and $q_{ij}^{p^{A-}}(t)$.

5. Results

In this section, we investigate the performance of the proposed vehicle–passenger matching method and evaluate the accuracy of the proposed dynamic model using a ride-sourcing benchmark developed in Aimsun microsimulation. In Fig. 5, the interaction between different modules of the developed benchmark is illustrated. The calibrated Aimsun microsimulation model of the city center of Barcelona (Kouvelas et al., 2017) is plugged into the benchmark. The studied network approximately covers an area of 8.21 squared kilometers containing 1570 sections and 721 junctions. The simulation lasts for 180 [min] in which 2500 ride-sourcing trip requests are considered. The Aimsun microscopic model includes other travel modes such as normal vehicles and public transport. The Aimsun microscopic model updates the model state (e.g., position of normal and ride-sourcing vehicles, passengers, and buses) every 0.5 [s]. In the following, first, we scrutinize the effects of the proposed vehicle–passenger matching method (see Section 3) in comparison with variants of the optimal myopic method. Subsequently, we assess the accuracy of the proposed model (see Section 4). The results of the designed controller for transferring idle vehicles are presented in the companion article.

5.1. Analysis of spatio-temporal filtering method

In this section, the proposed vehicle–passenger matching method is compared with optimal myopic and optimal myopic with greedy discarding under noticeable variations of vehicle supply and passenger demand. In the proposed matching method, spatio-temporal filtering method works in sequence after the optimal myopic matching to prune inefficient (long-distance) vehicle–passenger matchings. Note that vehicle transferring (repositioning) is not considered in this part to avoid reporting the intertwined effect of transferring with matching methods.

Fig. 6 illustrates the variation of the total number of passengers and ride-sourcing vehicles in 10 replications using the optimal myopic matching method, without considering impatient vehicles and drivers, with different random initializations for each replication. Furthermore, each replication contains considerable stochasticity in exogenous demand and supply rates. The exogenous demand and supply used in each replication are set to reflect time-varying patterns and under- and over-supply periods.

The optimal myopic method dispatches vehicles to the passengers by solving Eq. (1) in each matching instance without discarding long-distance matchings. This approach considers just the current state of the vehicles and passengers and is sensitive to a predefined matching interval. Moreover, it does not consider the effects of traffic congestion and the dynamics of idle vehicles and waiting passengers. Fig. 7 depicts the average of matching distances for different matching intervals. The results indicate that increasing the matching interval results in lower average and variance of vehicle–passenger matching distances (i.e., shorter vehicle's/passenger's reserved time). However, increasing the matching interval increases the unassigned time of vehicles and passengers, see Table 1.

Fig. 8 presents the average of matching distances using the matching with the greedy discarding method. The greedy method prunes the outcomes of the optimal myopic by discarding k long-distance vehicle–passenger matchings if they exceed the predefined distance threshold. This approach only considers the current number and location of passengers and vehicles. The illustrated results in Fig. 8 are obtained by choosing $k = 1$ and distance threshold of 900 [m]. The distance threshold is determined using a cut-off value of 99% for considering potential outlier matchings, see Fig. 7. The effectiveness of the greedy method is quantified in Table 1.

In the proposed vehicle–passenger matching method, the time-varying optimum values of the matching interval and the maximum matching distance are determined by solving Eq. (8) at each matching instance. Fig. 9 illustrates the number of waiting

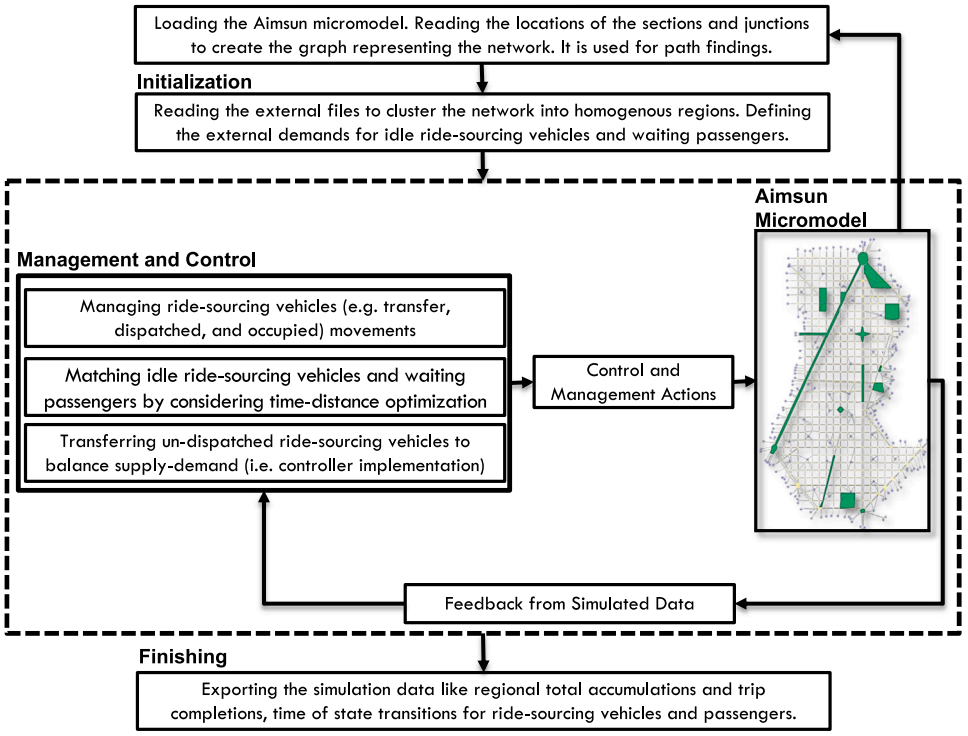

Fig. 5. Schematic interactions between the developed modules of the ride-sourcing microsimulation benchmark.

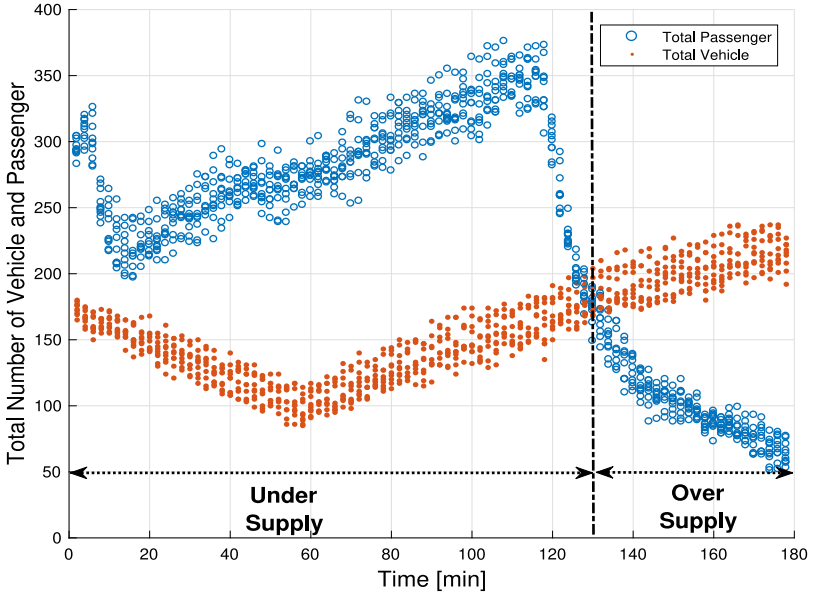

Fig. 6. The total number of passengers including waiting, assigned, and on-board and the total number of vehicles including idle, dispatched, and occupied in 10 replications.

passengers and idle vehicles in the network by implementing the adaptive spatio-temporal matching method. Fig. 10 elucidates how the matching interval and the number of discarded matchings are intertwined in the proposed method.

To analyze the results of the adaptive spatio-temporal matching method, we segment the three-hour simulation results in five time periods: (i) $\Delta t_1 \approx [0\text{ s}, 720\text{ s})$, (ii) $\Delta t_2 \approx [720\text{ s}, 2400\text{ s})$, (iii) $\Delta t_3 \approx [2400\text{ s}, 7200\text{ s})$, (iv) $\Delta t_4 \approx [7200\text{ s}, 8400\text{ s})$, and (v) $\Delta t_5 \approx [8400\text{ s}, 10\,800\text{ s}]$. In Δt_1, the number of waiting passengers is decreasing and is greater than the number of idle vehicles,

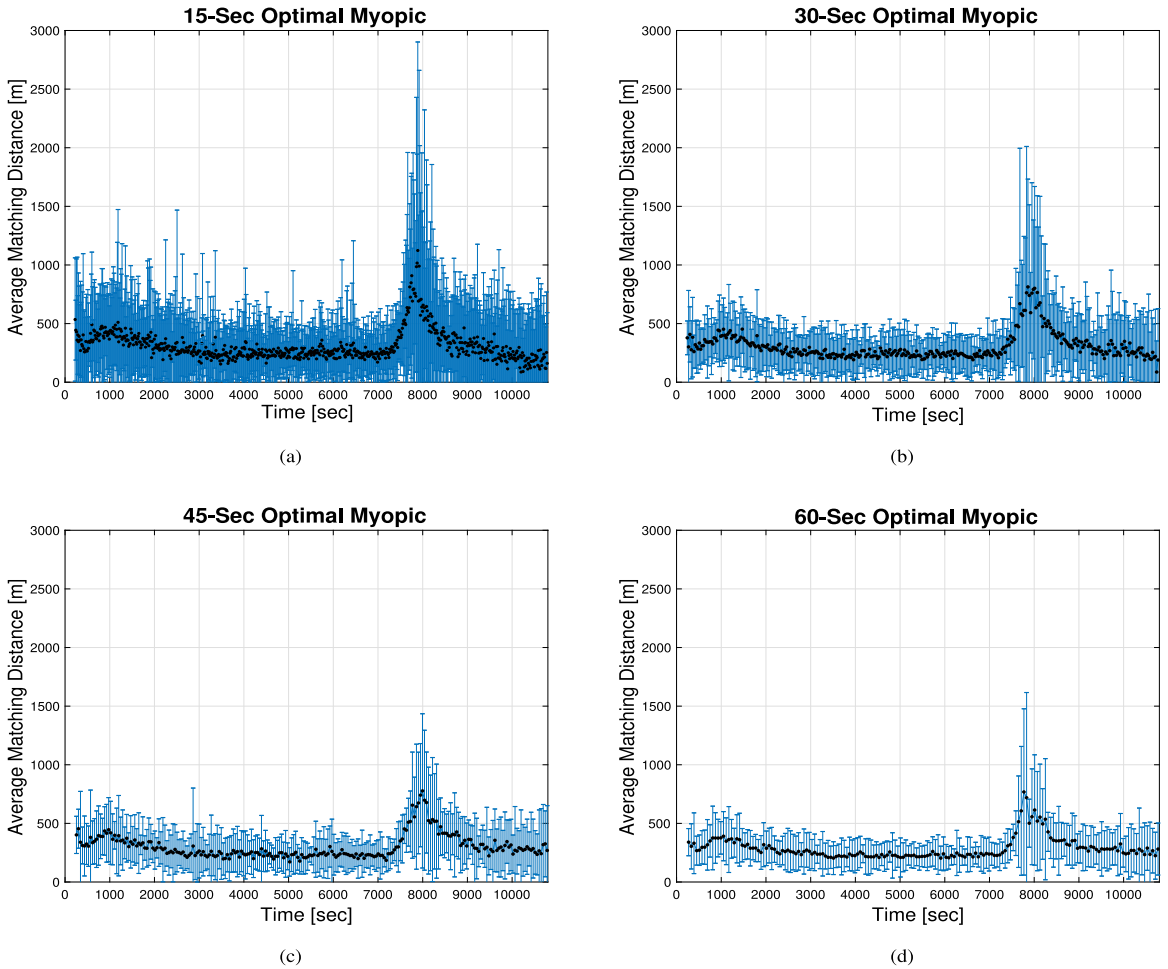

Fig. 7. Average of matching distances at each matching time using optimal myopic method with different matching intervals: (a) 15 s, (b) 30 s, (c) 45 s, and (d) 60 s. The bars represent 2.5% and 97.5% percentiles.

see Fig. 9. Hence, the average optimum matching distance based on Eq. (9) must be increasing as shown in Fig. 10 (a). The average matching distance moderately increases because the number of idle vehicles is *much less* than the number of waiting passengers. In this time period, the number of discarded matching is high and increasing, as shown in Figs. 10 (c), because the density of idle vehicles is low while the density of waiting passengers is decreasing. When the number of discarded matchings increases, the matching time interval decreases, as shown in Fig. 10 (d), to compensate for the delay caused by discarded matchings in the estimated total unassigned time (Eq. (3)) and the predicted total reserved time (Eq. (4)).

In $\Delta t_2 \approx [720\text{ s}, 2400\text{ s})$, the number of waiting passengers, which is greater than the number of idle vehicles, starts to increase while the number of idle vehicles does not change significantly, see Fig. 9. Hence, as expected based on Eq. (9), the average optimum matching distance decreases as in Fig. 10 (a). The number of idle vehicles is less than the number of waiting passengers, so the number of idle vehicles bounds the number of the matchings. On the other side, as the number of waiting passengers increases, the possibility of short-distance matchings is increased, which results in less discarded vehicle–passenger matching as illustrated in Figs. 10 (c). Furthermore, the optimum value of the next matching interval is increased, see Fig. 10 (d), to compensate for the effect of increasing the number of waiting passengers on the predicted total unassigned time (see Eq. (5)). Note that the method by increasing the matching interval generates fewer discarded matches. This is because longer matching intervals increase the number of idle vehicles and waiting passengers, which results in lower matching distances and discarding.

In $\Delta t_3 \approx [2400\text{ s}, 7200\text{ s})$, the numbers of idle vehicles and waiting passengers do not change notably. Hence, the average of matching distances, number of discarded matching, and matching intervals do not fluctuate significantly. The idle vehicles and waiting passengers trends in $\Delta t_4 \approx [7200\text{ s}, 8400\text{ s})$ are almost the same as Δt_1. Hence, the same explanation is valid. The idle vehicles and waiting passengers trends in $\Delta t_5 \approx [8400\text{ s}, 10\,800\text{ s}]$ are similar to Δt_2 if we use idle vehicles and waiting passengers interchangeably, because of the symmetric characteristic of the matching problem.

Table 1 presents the quantitative comparison of different matching methods. In this table, the total delay is the sum of reserved time and unassigned time for vehicles and passengers (including impatient passengers and drivers who leave the ride-sourcing

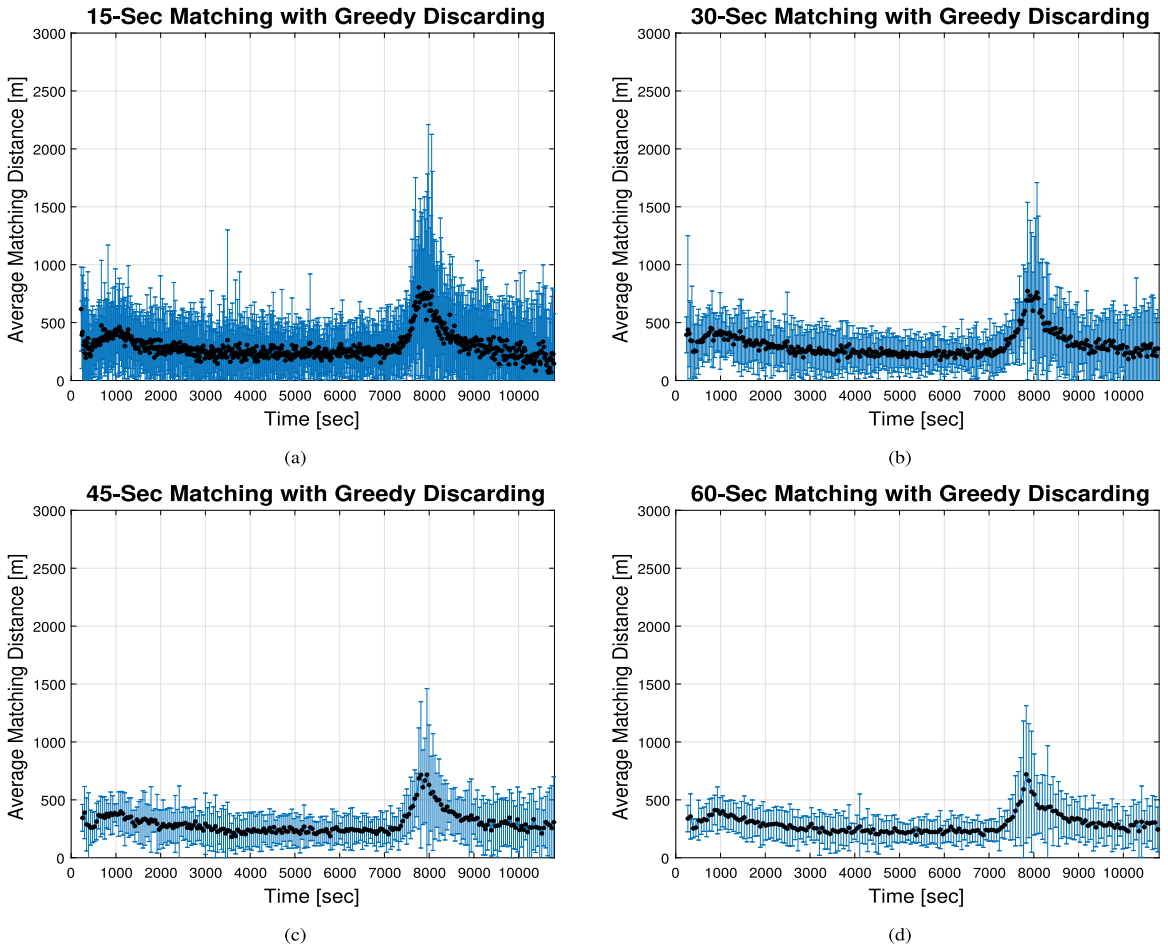

Fig. 8. Average of matching distances in each matching time using greedy discarding method with different matching intervals: (a) 15 s, (b) 30 s, (c) 45 s, and (d) 60 s. The bars represent 2.5% and 97.5% percentiles.

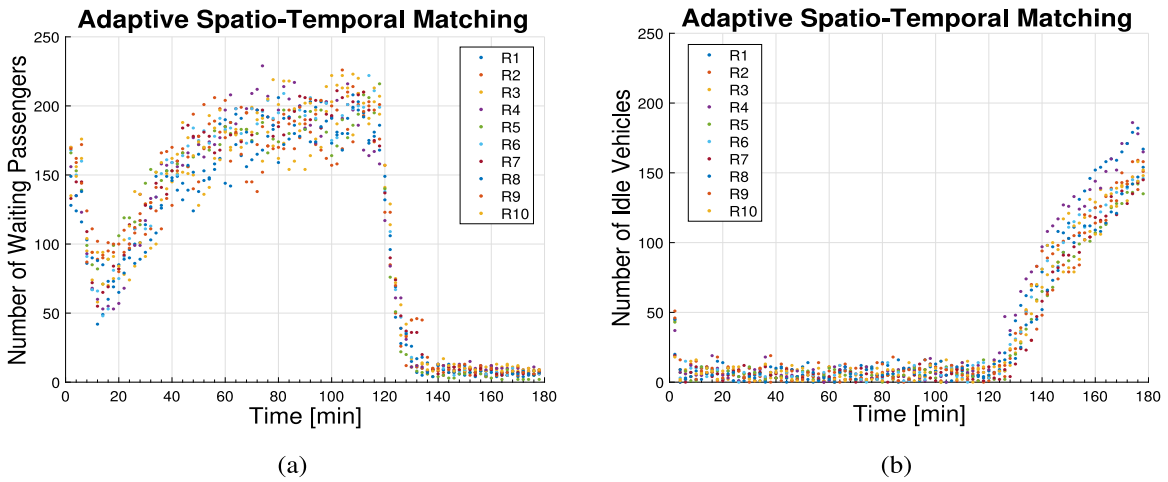

Fig. 9. (a) Total number of waiting passengers and (b) total number of idle vehicles by implementing the adaptive spatio-temporal matching method.

system.) Greater matching intervals decrease the average matching distance, reducing reserved time for vehicles and passengers. However, this inflates the unassigned time of passengers and vehicles. The proposed method shows significant improvement in

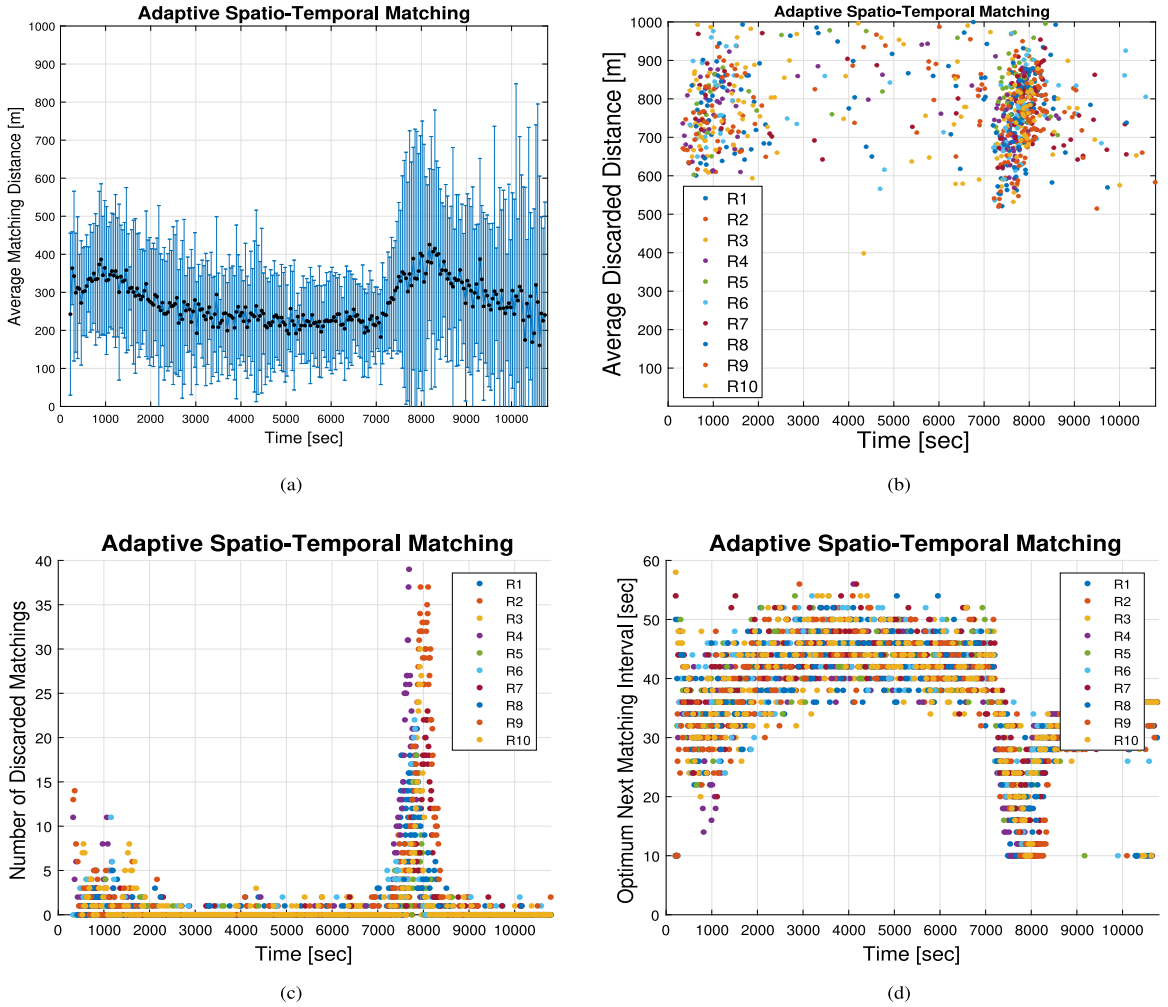

Fig. 10. Output of the adaptive spatio-temporal matching method: (a) average of matching distances after discarding, (b) average distance of discarded matchings, (c) number of discarded matchings, and (d) matching interval. The bars represent 2.5% and 97.5% percentiles and different dotted colors show different replications.

reducing total delay. It is worth pointing out that the unassigned times of the vehicles in 15-second optimal myopic and 15-second matching with greedy discarding are less than the proposed method because vehicles' unassigned time only considers the vehicles that are *successfully* matched to waiting passengers.

The number of (impatient) passengers who leave the network before boarding (i.e., order cancellations) for each method is reported in Table 1. These values are obtained by averaging over the ten replications. In these experiments, the patience times of passengers are selected from a normal distribution with a mean value of 600 [s] and a variance of 135 [s^2]. In addition, each driver's stochastic patience time threshold is randomly generated from a normal distribution with mean value of 1200 [s] and variance of 600 [s^2]. The number of order cancellations utilizing the adaptive spatio-temporal method is lower than greedy discarding and optimal myopic methods. Note that the total number of trip requests in each three-hour simulation replication is 2500. The numbers in parenthesis show the percentage of change with respect to the average of optimal myopic methods (matching intervals of 15, 30, 45, and 60 [s]).

As shown in Fig. 6, from time 0 [min] to 130 [min], the total number of ride-sourcing vehicles is less than the total number of passengers (i.e., under-supply period). The effect of the spatio-temporal matching method during this period is investigated in Table 2. In Table 3, the effect of the proposed method when the total number of ride-sourcing vehicles is greater than the total number of passengers, i.e., 130 [min] to 180 [min] (over-supply period), is evaluated. The comparison of Tables 2 and 3 reveals that the proposed method reduces the number of order cancellations, reserved time, passengers' unassigned time, and total delay in both under- and over-supply periods. For an under-supply market, the vehicles' unassigned time is almost equal to the average performance of optimal myopic methods; however, the passengers' unassigned time is reduced by 7.6%, and the order cancellation is reduced by 20.4%. It is noteworthy that the proposed method improves the quality of vehicle–passenger matchings more during the

Table 1
Comparison of adaptive spatio-temporal method and variants of optimal myopic methods concerning reserved time, unassigned time, total delay, and the number of order cancellations. The values are averaged over 10 replications. The matching interval for adaptive spatio-temporal method is time-varying and the reported value is the average of the matching intervals. The numbers in parenthesis represent the percentage of changes with respect to the average performances of optimal myopic method variants.

	Matching Interval [s]	Number of Order Cancellation	Passengers' Unassigned Time [s]		Vehicles' Unassigned Time [s]		Vehicles/Passengers Reserved Time [s]		Total Delay [s]	
			Mean	SD	Mean	SD	Mean	SD	Mean	SD
Optimal Myopic (No Discarding)	15	49.9	143.7	134.1	38.6	167.9	93.9	85.5	457.3	183.3
Optimal Myopic (No Discarding)	30	53.3	151.7	137.8	45.5	174.6	91.4	83.1	482.2	196.7
Optimal Myopic (No Discarding)	45	47.0	157.4	139.7	51.6	159.7	90.0	81.4	500.9	184.7
Optimal Myopic (No Discarding)	60	48.4	158.9	139.2	55.7	139.8	87.7	81.3	501.0	172.5
Matching with Greedy Discarding	15	49.5	143.4	135.2	38.2	157.8	91.8	82.7	458.0	183.5
Matching with Greedy Discarding	30	50.9	150.1	136.4	44.8	162.8	91.4	81.7	476.8	182.3
Matching with Greedy Discarding	45	42.4	155.3	138.0	51.2	157.1	88.8	79.8	489.9	181.0
Matching with Greedy Discarding	60	47.1	158.3	138.8	58.3	171.3	86.8	81.7	503.7	183.8
Adaptive Spatio-Temporal Method	34.8 (Mean)	38.8 (−21.9%)	143.0 (−6.5%)	128.1	48.1 (−0.5%)	159.0	80.6 (−11.2%)	74.3	371.2 (−23.5%)	158.4

Table 2
Comparison of adaptive spatio-temporal method and variants of optimal myopic methods with respect to the reserved time, unassigned time, total delay, and number of order cancellations for simulation time from 0 [min] to 130 [min] (i.e., under-supply period). The numbers in parenthesis represent the percentage of changes with respect to the average performances of optimal myopic method variants.

	Matching Interval [s]	Number of Order Cancellation	Passengers' Unassigned Time [s]		Vehicles' Unassigned Time [s]		Vehicles/Passengers Reserved Time [s]		Total Delay [s]	
			Mean	SD	Mean	SD	Mean	SD	Mean	SD
Optimal Myopic (No Discarding)	15	29.0	168.4	131.2	18.4	135.1	90.7	82.8	459.0	165.9
Optimal Myopic (No Discarding)	30	36.4	172.0	135.5	27.9	162.2	87.2	80.1	486.7	181.5
Optimal Myopic (No Discarding)	45	31.1	186.1	137.8	32.7	126.1	84.9	77.9	504.6	163.8
Optimal Myopic (No Discarding)	60	29.4	185.6	138.1	39.2	118.7	84.4	75.9	509.4	163.1
Matching with Greedy Discarding	15	34.7	172.6	132.3	18.8	128.7	87.9	79.9	460.7	164.2
Matching with Greedy Discarding	30	35.8	176.7	134.5	26.9	138.3	86.9	77.1	481.0	169.2
Matching with Greedy Discarding	45	28.1	182.2	136.6	33.9	145.0	85.1	75.4	496.4	172.5
Matching with Greedy Discarding	60	29.8	184.0	138.6	40.6	138.2	85.5	74.5	510.5	173.6
Adaptive Spatio-Temporal Method	36.0 (Mean)	25.3 (−20.4%)	164.8 (−7.6%)	130.3	29.8 (0.0%)	145.6	82.9 (−4.2%)	68.6	400.8 (−17.9%)	157.3

Table 3
Comparison of adaptive spatio-temporal method and variants of optimal myopic methods with respect to reserved time, unassigned time, total delay, and number of order cancellations for simulation time between 130 [min] to 180 [min] (i.e., over-supply period). The numbers in parenthesis represent the percentage of changes with respect to the average performances of optimal myopic method variants.

	Matching Interval [s]	Number of Order Cancellation	Passengers' Unassigned Time [s]		Vehicles' Unassigned Time [s]		Vehicles/Passengers Reserved Time [s]		Total Delay [s]	
			Mean	SD	Mean	SD	Mean	SD	Mean	SD
Optimal Myopic (No Discarding)	15	20.9	8.3	6.9	114.7	122.6	111.7	94.3	372.7	144.3
Optimal Myopic (No Discarding)	30	16.9	16.5	14.0	104.0	123.9	112.4	91.8	363.6	146.5
Optimal Myopic (No Discarding)	45	15.9	24.3	16.7	108.1	129.5	114.1	92.0	376.8	148.1
Optimal Myopic (No Discarding)	60	19.0	32.3	22.2	112.2	125.8	103.1	84.0	365.7	142.2
Matching with Greedy Discarding	15	14.8	9.7	11.3	107.1	123.7	111.6	91.0	355.7	142.4
Matching with Greedy Discarding	30	15.1	17.9	15.11	102.7	131.2	113.9	88.2	367.3	151.0
Matching with Greedy Discarding	45	14.3	24.1	16.6	109.6	128.5	106.9	83.0	363.6	140.6
Matching with Greedy Discarding	60	17.3	33.4	24.2	113.9	126.1	104.8	83.7	376.8	150.4
Adaptive Spatio-Temporal Method	33.1 (Mean)	13.5 (−19.5%)	15.9 (−29.3%)	14.7	97.7 (−10.4%)	128.8	93.0 (−4.4%)	72.0	316.8 (−13.8%)	113.2

under-supply period. This supports the conjecture that the effect of matching algorithms on the system efficiency can be manifested more in under-supplied markets because matching algorithms can enable the efficient use of resources.

5.2. Model validation

Traffic congestion is heterogeneous in the case study, which results in MFDs with noticeable scatter. As the developed formulations are based on MFDs, we need to partition the network into homogeneous regions to observe well-defined low-scatter MFDs. Fig. 11 (a) depicts the partitioning of the network into four homogeneous regions as suggested in Kouvelas et al. (2017) and Sirmatel et al. (2021). To validate the proposed model, we consider inter-regional flows for ride-sourcing vehicles (i.e., transfer, dispatched, and occupied) and passengers (i.e., assigned) between neighbor regions. We do not consider flows from/to non-neighboring regions because the matching algorithm prevents long-distance matchings between idle/transfer ride-sourcing vehicles and waiting passengers in faraway regions. In addition, the travel requests are defined for the neighboring regions (that is, the destination of the request is not in a non-neighboring region). This assumption is not very limiting for the case study microsimulation network as Regions 1, 2, and 3 are not directly connected. Region 4 is the central region, and the other regions are peripheral. We consider the ride-sourcing travel requests from the central region to the peripheral regions and vice versa. However, in real practice,

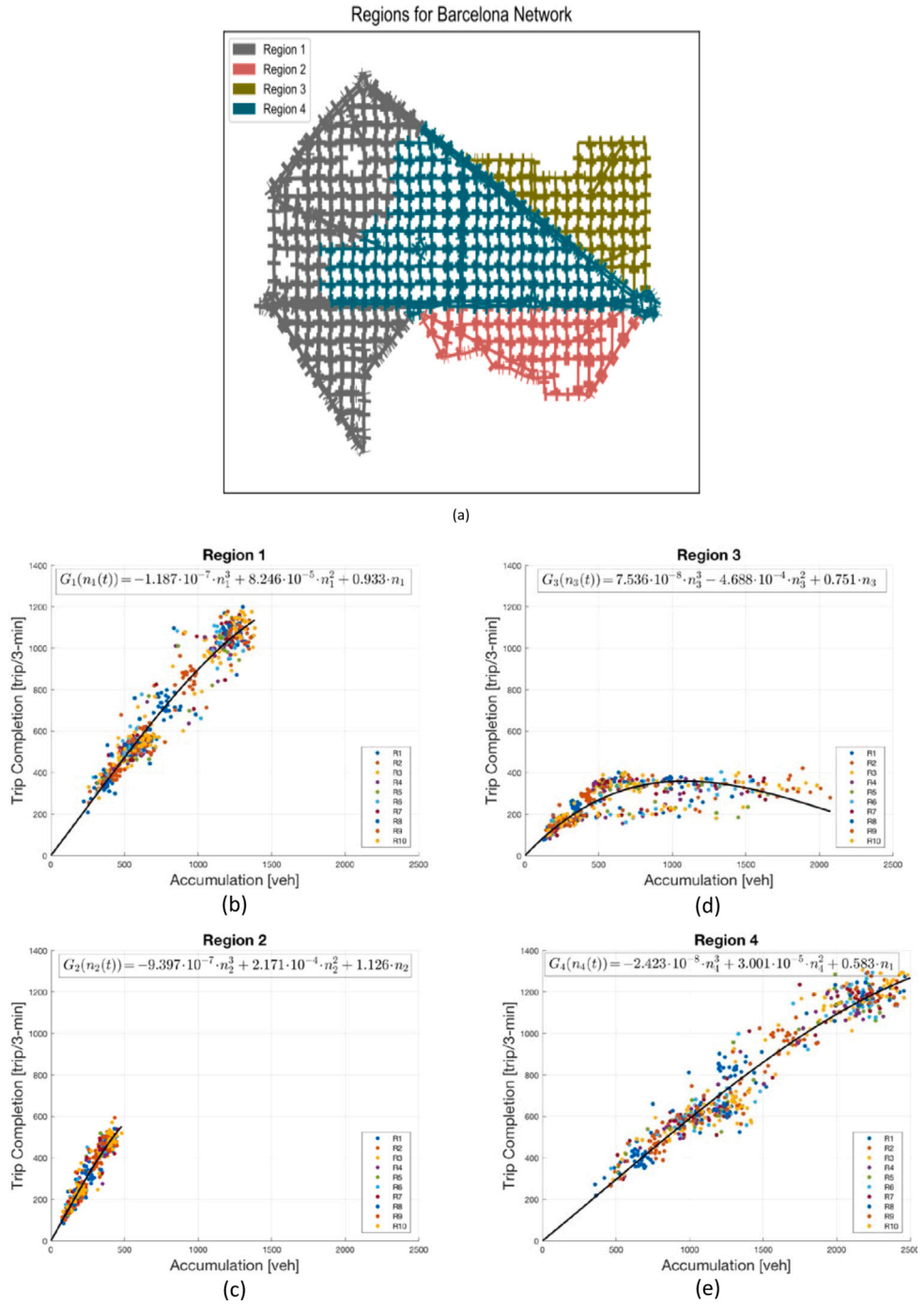

Fig. 11. (8) Homogeneous regions of the city center of Barcelona. Macroscopic Fundamental Diagram (MFD) for (b) Region 1, (c) Region 2, (d) Region 3, and (e) Region 4. n_i denotes the total accumulation including buses, ride-sourcing vehicles, and normal vehicles in Region i. Trip completion rate in Region i is denoted by G_i. The solid lines show the estimated MFD functions. The dotted colors illustrate the simulation results of different replications.

with different topology of regions, a general form of origins and destinations of ride-sourcing trips should be considered. This would require defining more traffic states, which is a straightforward yet cumbersome extension of the proposed macro model.

We run the microsimulation model with different demand levels and initial states to obtain the regional MFDs. Figs. 11 (b) to 11 (e) illustrate the simulated and estimated MFD functions. Different colors distinguish the results of different replications. The

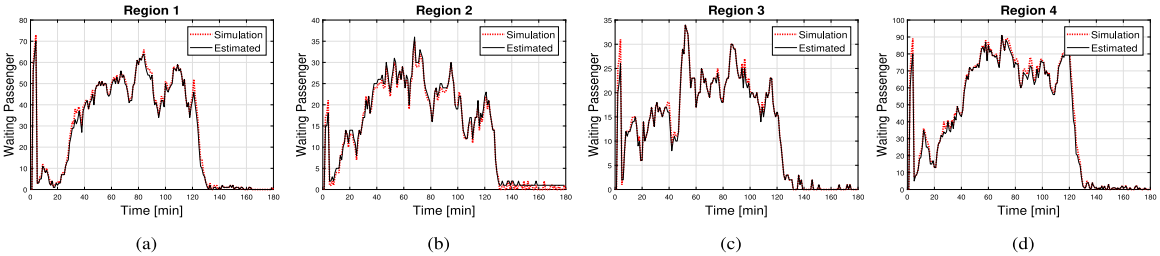

Fig. 12. Comparison of estimated and simulated evolution of the number of waiting passengers for: (a) Region 1, (b) Region 2, (c) Region 3, and (d) Region 4. The black solid lines show the estimated values of regional waiting passengers. The red dotted lines illustrate the simulation results.

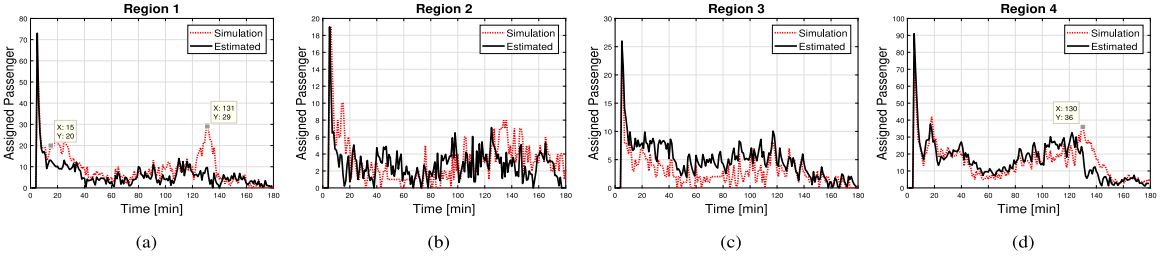

Fig. 13. Comparison of estimated and simulated evolution of the number of assigned passengers for: (a) Region 1, (b) Region 2, (c) Region 3, and (d) Region 4. The black solid lines show the estimated values of regional assigned passengers. The red dotted lines illustrate the simulation results.

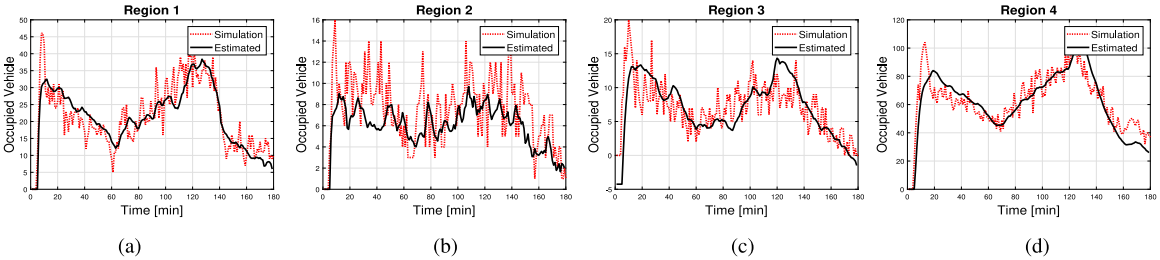

Fig. 14. Comparison of estimated and simulated evolution of the number of occupied vehicles for: (a) Region 1, (b) Region 2, (c) Region 3, and (d) Region 4. The black solid lines show the estimated values of regional occupied vehicles. The red dotted lines illustrate the simulation results.

solid lines represent the estimated MFDs with the constrained least square method based on the simulated data. We use the estimated MFDs in evaluating the proposed ride-sourcing model.

Figs. 12 to 16 assess the accuracy of the proposed macroscopic model of the ride-sourcing system with the adaptive spatio-temporal matching method as the dispatching subsystem. This model validation aims to study the accuracy of macroscopic aggregation of boarding rate with Cobb–Douglas meeting function in Eq. (10), homogeneity assumption in Eq. (11), and MFD dynamics in Eqs. (12) to (16). Fig. 12 depicts the estimated number of waiting passengers (Eqs. (24) and (25)) and the simulated number of waiting passengers with dotted red lines. Root mean square error (RMSE) of estimated waiting passengers for regions 1 to 4 are: 1.51, 0.88, 0.82, and 2.17, respectively. The estimated values closely follow the simulated values because the exogenous terms are dominant in estimating the number of waiting passengers in each region.

For model validation reported in these figures, two sets of information are fed to the model in addition to the exogenous inputs (i.e., the arrival rate of idle vehicles and waiting passengers): initial values of states and the rate of vehicle–passenger matchings. The main sources of uncertainties in the model are (i) the initial location of new arriving idle vehicles and new passengers in each region, (ii) stochastic thresholds of patience time of passengers and drivers, and (iii) cruising movements of idle vehicles. Figs. 12 and 16 show higher accuracy as the evolution of the waiting passengers and idle vehicles are dominated by exogenous inputs. The model cannot capture the abrupt variations in the number of assigned passengers and occupied vehicles (see Figs. 13 and 14). This is because these states are estimated chiefly by MFD functions that are more valid under slow-varying conditions.

The estimated number of assigned passengers, based on Eqs. (26) and (27), and simulated number of assigned passengers in regions 1–4 are compared in Fig. 13. The initial peaks in this Figure are due to the high number of idle vehicles and waiting passengers that are considered in the matching procedure at the beginning of the simulation. The RMSE of estimated number of assigned passengers of regions 1 to 4 are: 5.66, 2.61, 2.59, and 8.42, respectively. Cobb–Douglas matching function that is used in

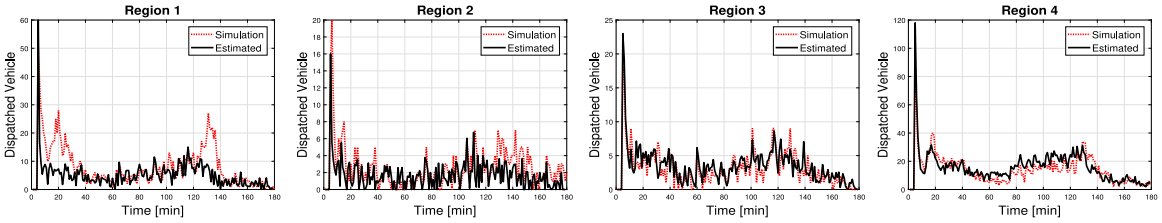

Fig. 15. Comparison of estimated and simulated evolution of the number of dispatched vehicles for: (a) Region 1, (b) Region 2, (c) Region 3, and (d) Region 4. The black solid lines show the estimated values of regional dispatched vehicles. The red dotted lines illustrate the simulation results.

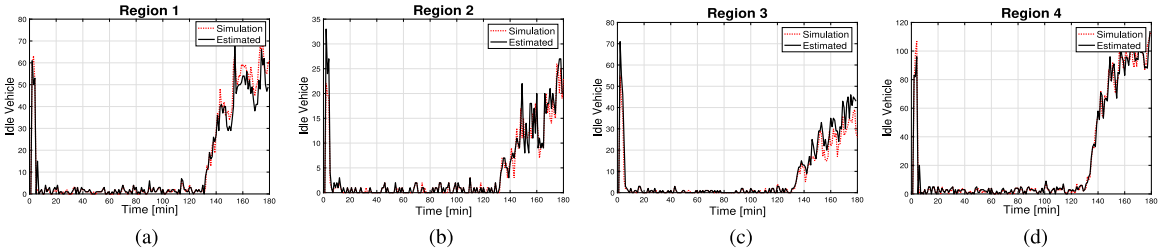

Fig. 16. Comparison of estimated and simulated evolution of the number of idle vehicles for: (a) Region 1, (b) Region 2, (c) Region 3, (d) Region 4. The black solid lines show the estimated values of regional idle vehicles. The red dotted lines illustrate the simulation results.

Eqs. (26) and (27) cannot accurately capture the number of assigned passengers when there are abrupt changes in the total number of passengers (e.g., 15 [min] and 130 [min]), as shown in Fig. 6.

RMSE for estimated number of occupied vehicles (see Fig. 14), based on Eqs. (17) and (18), in regions 1 to 4 are: 4.86, 3.04, 3.24, and 8.57. The occupied vehicles are intrinsically a slow-varying component of ride-sourcing systems, so they can be accurately estimated using MFDs and Cobb–Douglas functions. RMSE for estimated dispatched vehicles, based on Eqs. (19) and (20), in regions 1 to 4 are: 4.20, 8.21, 1.57, and 6.31, respectively. The estimated and the simulated number of dispatched vehicles are depicted in Fig. 15. Similar to assigned passengers, the number of dispatched vehicles is dominated by the results of the dispatching subsystem which lead to high variations.

Fig. 16 illustrates the comparison of the estimated idle vehicles, based on Eq. (23), and simulated idle vehicles. RMSE for estimation of idle vehicles are: 3.93, 2.08, 4.06, and 4.39 for regions 1 to 4, respectively.

6. Summary and future research

This article has presented a dynamic macroscopic model and a matching method for ride-sourcing systems. The macroscopic dynamical ride-sourcing model is developed for a network partitioned into a number of homogeneous regions and tracks the spatio-temporal evolution of different states of ride-sourcing vehicles (i.e., transferred, idle, dispatched, and occupied) and passengers (i.e., waiting and assigned) between regions. Impatient passengers and drivers are considered in the proposed model endogenously. The non-equilibrium macroscopic model is built upon the Macroscopic Fundamental Diagram (MFD) and Cobb–Douglas matching function. Contrary to the conventional approaches, we proposed a non-equilibrium model that overcomes the limitation of stationary and steady-state analysis of the ride-sourcing systems. The model provides the capabilities of considering vehicle–passenger matching scenarios and designing a controller to reposition idle ride-sourcing vehicles. The proposed macroscopic model is evaluated with micro-level data utilizing a microsimulation benchmark of ride-sourcing systems. A Nonlinear Model Predictive Controller is developed in Part II based on the model constructed in Part I of this study.

In addition to the proposed ride-sourcing model, we proposed an algorithm to dynamically determine the optimum matching intervals and maximum matching distance to minimize passengers' waiting time. The algorithm considered (i) the intertwined effect of matching time interval and maximum matching distance, (ii) level of congestion of the network, and (iii) dynamics of waiting passengers and idle/transferred vehicles to find the optimum values at each matching time instance. The validity of the macroscopic model and the benefits of the matching method have been demonstrated with microsimulation.

Several future research directions are envisaged. The passengers and ride-sourcing vehicles arrival profiles can be modeled elastic (in the short-term) to the market conditions (e.g. passengers' and vehicle's waiting time). This will lead to positive and negative short-term induced demand and supply that requires more behavioral research on both sides of the market (Ramezani et al., 2022). Furthermore, speed as an indicator of network congestion is considered an exogenous factor. Integrating the network congestion indicator estimation from the ride-sourcing fleet (e.g., as probe vehicles) is another future research direction. Moreover, the effect of competition between ride-sourcing companies on vehicle–passenger matching and repositioning is a challenging future study. The

proposed matching method relies on solving the matching problem of a bipartite graph. Scaling this to obtain the exact solution is a challenge that requires further research (Bertsimas et al., 2019). Furthermore, extending the proposed framework, method, and model to ride-splitting (ride-sharing) (e.g., see Jiao and Ramezani, 2022) is a research priority.

CRediT authorship contribution statement

Mohsen Ramezani: Conceptualization, Methodology, Validation, Formal analysis, Investigation, Writing – original draft, Writing – review & editing, Supervision. **Amir Hosein Valadkhani:** Methodology, Software, Validation, Formal analysis, Investigation, Data curation, Writing – original draft.

Acknowledgments

The authors thank the three anonymous reviewers for their valuable comments that improved the rigor and quality of the manuscript. This research was partially funded by the Australian Research Council (ARC) Discovery Early Career Researcher Award (DECRA) DE210100602.

Appendix. Nomenclature

Sets	
$\mathbb{R}$	Set of homogeneous regions
$\mathbb{U}_i$	Set of regions in the vicinity of Region i
Functions	
$b_{ij}(t)$	Vehicle boarding rate from Region i to Region j at time t
P_i	Total trip production (MFD) in Region i
Parameters	
$l_{ij}^{\mathrm{O}}(t)$	Average trip length of occupied vehicles in Region i with destination in Region j at time t
$l_{ij}^{\mathrm{T}}(t)$	Average trip length of transferred vehicles in Region i with destination in Region j at time t
$l_{ij}^{\mathrm{D}}(t)$	Average trip length of dispatched vehicles in Region i with destination in Region j at time t
α_i	Boarding function elasticity with respect to the number of dispatched vehicles in Region i
β_i	Boarding function elasticity with respect to the number of assigned passengers in Region i
γ_i	Boarding function elasticity with respect to average speed of Region i
K_i	Total productivity of boarding function in Region i
Variables	
$\hat{T}_{\mathrm{R}}(t_{\mathrm{m}}^{\iota})$	Estimated total reserved time of matchings at t_{m}^{ι}
$\hat{T}_{\mathrm{D}}(t_{\mathrm{m}}^{\iota})$	Estimated total unassigned time of the waiting passengers at t_{m}^{ι}
$\hat{T}_{\mathrm{R}}(t_{\mathrm{m}}^{\iota+1})$	Predicted total reserved time for matchings at $t_{\mathrm{m}}^{\iota+1}$
$\hat{T}_{\mathrm{D}}(t_{\mathrm{m}}^{\iota+1})$	Predicted total unassigned time for waiting passengers at $t_{\mathrm{m}}^{\iota+1}$
$\hat{T}_{\mathrm{P}}^{t_{\mathrm{m}}^{\iota+1}-t_{\mathrm{m}}^{\iota}}$	Expected total passengers' waiting time during interval $[t_{\mathrm{m}}^{\iota}, t_{\mathrm{m}}^{\iota+1})$
$m(t_{\mathrm{m}}^{\iota})$	Number of matchings before discarding of long-distance matchings at t_{m}^{ι}
$\bar{l}_r(t_{\mathrm{m}}^{\iota})$	Average distance of optimal matchings after discarding at t_{m}^{ι}
$\hat{\bar{l}}_r(t_{\mathrm{m}}^{\iota+1})$	Prediction of average matching distance
$r(t_{\mathrm{m}}^{\iota})$	Number of long-distance vehicle–passenger discardings at t_{m}^{ι}
$\rho_{\mathrm{c}}(t_{\mathrm{m}}^{\iota})$	Total arrival rate of idle/transferred vehicles during interval $[t_{\mathrm{m}}^{\iota}, t_{\mathrm{m}}^{\iota+1})$
$\rho_{\mathrm{p}}(t_{\mathrm{m}}^{\iota})$	Total arrival rate of waiting passengers during interval $[t_{\mathrm{m}}^{\iota}, t_{\mathrm{m}}^{\iota+1})$
$t_{\mathrm{m}}^{\max}$	Upper bound for the next matching time instance
$c_{ij}^{\mathrm{O}}(t)$	Number of occupied vehicles in Region i with destination in Region j at time t
$c_{ij}^{\mathrm{T}}(t)$	Number of transferred vehicles in Region i with destination in Region j at time t
$c_{ij}^{\mathrm{D}}(t)$	Number of dispatched vehicles in Region i with destination in Region j at time t
$c_i^{\mathrm{I}}(t)$	Number of idle vehicles in Region i time t
$p_{ij}^{\mathrm{W}}(t)$	Number of waiting passengers in Region i with destination in Region j at time t
$p_{ij}^{\mathrm{A}}(t)$	Number of assigned passengers in Region i with destination in Region j at time t
$M_{ij}^{\mathrm{O}}(t)$	Occupied vehicle inter-region flow between Region i and Region j at time t
$M_{ij}^{\mathrm{T}}(t)$	Transferred vehicle inter-region flow between Region i and Region j at time t
$M_{ij}^{\mathrm{D}}(t)$	Dispatched vehicle inter-region flow between Region i and Region j at time t
$M_{ii}^{\mathrm{O}}(t)$	Occupied vehicle internal flow in Region i at time t
$M_{ii}^{\mathrm{T}}(t)$	Transferred vehicle internal flow in Region i at time t
$v_i(t)$	Average speed of Region i

$\hat{v}(t_{\mathrm{m}}^{t})$	Estimated network average speed at time t_{m}^{t}
$W_{ij}^{\mathrm{I\text{-}D}}(t)$	Rate of idle vehicles in Region i that are dispatched to Region j
$W_{ij}^{\mathrm{T\text{-}D}}(t)$	Rate of transferred vehicles in Region i that are dispatched to Region j
$W_{ij}^{\mathrm{I\text{-}T}}(t)$	Rate of idle vehicles in Region i that transfer to Region j
$W_{ij}^{\mathrm{W\text{-}A}}(t)$	Rate of waiting passengers which become assigned in Region i with destination in j at time t
R_{ij}^{D}	Rate of cancellation of dispatched trips in Region i with destination in j at time t
$w_i^{\mathrm{I}}(t)$	Rate of idle vehicles that enter (or leave) Region i at time t because of their random cruising
$q_i^{c+}(t)$	Rate of idle ride-sourcing vehicles exogenously enter to the network in Region i at time t
$q_i^{c-}(t)$	Rate of idle ride-sourcing vehicles leave the network from Region i at time t
$q_{ij}^{pW+}(t)$	Exogenous rate of waiting passenger demand in Region i going to Region j at time t
$q_{ij}^{pW-}(t)$	Leaving rate of impatient unassigned passengers in Region i with final destination in Region j at time t
$q_{ij}^{pA-}(t)$	Leaving rate of impatient assigned passengers in Region i with trip destination in Region j at time t

References

Agatz, N., Erera, A.L., Savelsbergh, M.W., Wang, X., 2011. Dynamic ride-sharing: A simulation study in metro Atlanta. Procedia-Soc. Behav. Sci. 17, 532–550.

Agatz, N., Erera, A., Savelsbergh, M., Wang, X., 2012. Optimization for dynamic ride-sharing: A review. European J. Oper. Res. 223 (2), 295–303.

Alisoltani, N., Leclercq, L., Zargayouna, M., 2021. Can dynamic ride-sharing reduce traffic congestion? Transp. Res. B 145, 212–246.

Beojone, C.V., Geroliminis, N., 2021. On the inefficiency of ride-sourcing services towards urban congestion. Transp. Res. C 124, 102890.

Bertsimas, D., Jaillet, P., Martin, S., 2019. Online vehicle routing: The edge of optimization in large-scale applications. Oper. Res. 67 (1), 143–162.

Castillo, J.C., Knoepfle, D., Weyl, G., 2017. Surge pricing solves the wild goose chase. In: Proceedings of the 2017 ACM Conference on Economics and Computation. pp. 241–242.

Chen, L., Valadkhani, A.H., Ramezani, M., 2021. Decentralised cooperative cruising of autonomous ride-sourcing fleets. Transp. Res. C 131, 103336.

Dandl, F., Hyland, M., Bogenberger, K., Mahmassani, H.S., 2019. Evaluating the impact of spatio-temporal demand forecast aggregation on the operational performance of shared autonomous mobility fleets. Transportation 46 (6), 1975–1996.

Douglas, G.W., 1972. Price regulation and optimal service standards: The taxicab industry. J. Transp. Econ. Policy 116–127.

Geroliminis, N., Daganzo, C.F., 2008. Existence of urban-scale macroscopic fundamental diagrams: Some experimental findings. Transp. Res. B 42 (9), 759–770.

Haddad, J., Zheng, Z., 2020. Adaptive perimeter control for multi-region accumulation-based models with state delays. Transp. Res. B 137, 133–153.

Ho, S.C., Szeto, W., Kuo, Y.-H., Leung, J.M., Petering, M., Tou, T.W., 2018. A survey of dial-a-ride problems: Literature review and recent developments. Transp. Res. B 111, 395–421.

Hörl, S., Ruch, C., Becker, F., Frazzoli, E., Axhausen, K.W., 2019. Fleet operational policies for automated mobility: A simulation assessment for Zurich. Transp. Res. C 102, 20–31.

Hu, L., Dong, J., 2020. An artificial-neural-network-based model for real-time dispatching of electric autonomous taxis. IEEE Trans. Intell. Transp. Syst..

Hyland, M., Mahmassani, H.S., 2018. Dynamic autonomous vehicle fleet operations: Optimization-based strategies to assign AVs to immediate traveler demand requests. Transp. Res. C 92, 278–297.

Ingole, D., Mariotte, G., Leclercq, L., 2020. Perimeter gating control and citywide dynamic user equilibrium: A macroscopic modeling framework. Transp. Res. C 111, 22–49.

Jiao, G., Ramezani, M., 2022. Incentivizing shared rides in e-hailing markets: Dynamic discounting. Transp. Res. C 144, 103879.

Kouvelas, A., Saeedmanesh, M., Geroliminis, N., 2017. Enhancing model-based feedback perimeter control with data-driven online adaptive optimization. Transp. Res. B 96, 26–45.

Lagos, R., 2000. An alternative approach to search frictions. J. Polit. Econ. 108 (5), 851–873.

Li, Y., Mohajerpoor, R., Ramezani, M., 2021. Perimeter control with real-time location-varying cordon. Transp. Res. B 150, 101–120.

Mahmassani, H.S., Saberi, M., Zockaie, A., 2013. Urban network gridlock: Theory, characteristics, and dynamics. Procedia-Soc. Behav. Sci. 80, 79–98.

Manski, C.F., Wright, J.D., 1967. Nature of equilibrium in the market for taxi services. Technical Report.

Nourinejad, M., Ramezani, M., 2019. Ride-sourcing modeling and pricing in non-equilibrium two-sided markets. Transp. Res. B.

Orr, D., 1969. The "Taxicab problem": A proposed solution. J. Polit. Econ. 77 (1), 141–147.

Qian, X., Ukkusuri, S.V., 2017. Taxi market equilibrium with third-party hailing service. Transp. Res. B 100, 43–63.

Ramezani, M., Haddad, J., Geroliminis, N., 2015. Dynamics of heterogeneity in urban networks: aggregated traffic modeling and hierarchical control. Transp. Res. B 74, 1–19.

Ramezani, M., Nourinejad, M., 2018. Dynamic modeling and control of taxi services in large-scale urban networks: A macroscopic approach. Transp. Res. C 94, 203–219.

Ramezani, M., Yang, Y., Elmasry, J., Tang, P., 2022. An empirical study on characteristics of supply in e-hailing markets: a clustering approach. Transp. Lett. 1–14.

Saeedmanesh, M., Geroliminis, N., 2016. Clustering of heterogeneous networks with directional flows based on "Snake" similarities. Transp. Res. B 91, 250–269.

Salanova, J.M., Estrada, M., Aifadopoulou, G., Mitsakis, E., 2011. A review of the modeling of taxi services. Procedia-Soc. Behav. Sci. 20, 150–161.

Santi, P., Resta, G., Szell, M., Sobolevsky, S., Strogatz, S.H., Ratti, C., 2014. Quantifying the benefits of vehicle pooling with shareability networks. Proc. Natl. Acad. Sci. 111 (37), 13290–13294.

Sirmatel, I.I., Tsitsokas, D., Kouvelas, A., Geroliminis, N., 2021. Modeling, estimation, and control in large-scale urban road networks with remaining travel distance dynamics. Transp. Res. C 128, 103157.

Vazifeh, M.M., Santi, P., Resta, G., Strogatz, S., Ratti, C., 2018. Addressing the minimum fleet problem in on-demand urban mobility. Nature 557 (7706), 534.

Vazirani, V.V., 1994. A theory of alternating paths and blossoms for proving correctness of the $O(\sqrt{V}E)$ general graph maximum matching algorithm. Combinatorica 14 (1), 71–109.

Wang, X., Agatz, N., Erera, A., 2017. Stable matching for dynamic ride-sharing systems. Transp. Sci. 52 (4), 850–867.

Wang, H., Yang, H., 2019. Ridesourcing systems: A framework and review. Transp. Res. B 129, 122–155.

Wong, R., Szeto, W., Wong, S., 2015. A two-stage approach to modeling vacant taxi movements. Transp. Res. Procedia 7, 254–275.

Wong, K., Wong, S., Bell, M., Yang, H., 2005. Modeling the bilateral micro-searching behavior for urban taxi services using the absorbing markov chain approach. J. Adv. Transp. 39 (1), 81–104.

Wong, K., Wong, S., Yang, H., 2001. Modeling urban taxi services in congested road networks with elastic demand. Transp. Res. B 35 (9), 819–842.

Xu, Z., Yin, Y., Ye, J., 2020. On the supply curve of ride-hailing systems. Transp. Res. B 132, 29–43.

Yang, H., Fung, C., Wong, K.I., Wong, S., 2010a. Nonlinear pricing of taxi services. Transp. Res. A 44 (5), 337–348.

Yang, H., Leung, C.W., Wong, S., Bell, M.G., 2010b. Equilibria of bilateral taxi–customer searching and meeting on networks. Transp. Res. B 44 (8–9), 1067–1083.
Yang, H., Qin, X., Ke, J., Ye, J., 2020. Optimizing matching time interval and matching radius in on-demand ride-sourcing markets. Transp. Res. B 131, 84–105.
Yang, Y., Ramezani, M., 2023. A learning method for real-time repositioning in E-hailing services. IEEE Trans. Intell. Transp. Syst. 24 (2), 1644–1654.
Yang, H., Wong, S., 1998. A network model of urban taxi services. Transp. Res. B 32 (4), 235–246.
Yang, H., Yang, T., 2011. Equilibrium properties of taxi markets with search frictions. Transp. Res. B 45 (4), 696–713.
Zha, L., Yin, Y., Xu, Z., 2018. Geometric matching and spatial pricing in ride-sourcing markets. Transp. Res. C 92, 58–75.
Zha, L., Yin, Y., Yang, H., 2016. Economic analysis of ride-sourcing markets. Transp. Res. C 71, 249–266.
Zhan, X., Qian, X., Ukkusuri, S.V., 2016. A graph-based approach to measuring the efficiency of an urban taxi service system. IEEE Trans. Intell. Transp. Syst. 17 (9), 2479–2489.
Zhang, K., Chen, H., Yao, S., Xu, L., Ge, J., Liu, X., Nie, M., 2019. An efficiency paradox of uberization. Available At SSRN 3462912.
Zheng, N., Waraich, R.A., Axhausen, K.W., Geroliminis, N., 2012. A dynamic cordon pricing scheme combining the macroscopic fundamental diagram and an agent-based traffic model. Transp. Res. A 46 (8), 1291–1303.